

# TOP-ERL: TRANSFORMER-BASED OFF-POLICY EPISODIC REINFORCEMENT LEARNING

**Anonymous authors**

Paper under double-blind review

## ABSTRACT

This work introduces Transformer-based Off-Policy Episodic Reinforcement Learning (TOP-ERL), a novel algorithm that enables off-policy updates in the ERL framework. In ERL, policies predict entire action trajectories over multiple time steps instead of single actions at every time step. These trajectories are typically parameterized by trajectory generators such as Movement Primitives (MP), allowing for smooth and efficient exploration over long horizons while capturing high-level temporal correlations. However, ERL methods are often constrained to on-policy frameworks due to the difficulty of evaluating state-action values for entire action sequences, limiting their sample efficiency and preventing the use of more efficient off-policy architectures. TOP-ERL addresses this shortcoming by segmenting long action sequences and estimating the state-action values for each segment using a transformer-based critic architecture alongside an n-step return estimation. These contributions result in efficient and stable training that is reflected in the empirical results conducted on sophisticated robot learning environments. TOP-ERL significantly outperforms state-of-the-art RL methods. Thorough ablation studies additionally show the impact of key design choices on the model performance. Our code is available at an anonymous link [https://github.com/toperliclr2025/TOP\\_ERL.git](https://github.com/toperliclr2025/TOP_ERL.git).

## 1 INTRODUCTION

This work introduces a novel off-policy Reinforcement Learning (RL) algorithm that utilizes a transformer-based architecture for predicting the state-action values for a sequence of actions. These returns are effectively used to update the policy that predicts a smooth trajectory instead of a single action in each decision step. Predicting a whole trajectory of actions is commonly done in episodic RL (ERL) (Kober & Peters, 2008) and differs conceptually from conventional step-based RL (SRL) methods like PPO (Schulman et al., 2017) and SAC (Haarnoja et al., 2018a) where an action is sampled in each time step. The action selection concept in ERL is promising as shown in recent works in RL (Otto et al., 2022; Li et al., 2024). Similar insights have been made in the field of Imitation Learning, where predicting action sequences instead of single actions has led to great success (Zhao et al., 2023; Reuss et al., 2024). Additionally, decision-making in ERL aligns with the human’s decision-making strategy, where the human generally does not decide in each single time step but rather performs a whole sequence of actions to complete a task – for instance, swinging an arm to play tennis without overthinking each per-step movement.

**Episodic RL** is a distinct family of RL that emphasizes the maximization of returns over entire episodes, typically lasting several seconds, rather than optimizing the intermediate states during environment interactions (Whitley et al., 1993; Igel, 2003; Peters & Schaal, 2008). Unlike SRL, ERL shifts the solution search from per-step actions to a parameterized trajectory space, leveraging techniques like Movement Primitives (MPs) (Schaal, 2006; Paraschos et al., 2013) for generating action sequences. This approach enables a broader exploration horizon (Kober & Peters, 2008), captures temporal and degrees of freedom (DoF) correlations (Li et al., 2024), and ensures smooth transitions between re-planning phases (Otto et al., 2023). Recent advances have integrated ERL with deep learning architectures, demonstrating significant potential in areas such as versatile skill acquisition (Celik et al., 2024) and safe robot reinforcement learning (Kicki et al., 2024). However, despite their advantages, ERL methods often suffer from low update efficiency. Nearly all ERL approaches to date remain constrained to an on-policy training paradigm, limiting their ability to

exploit more efficient off-policy update rules, where an action-value function, or *critic*, is explicitly learned to guide policy updates and action selection. The primary challenge is that prominent off-policy methods, such as SAC (Haarnoja et al., 2018a), rely on temporal difference (TD) error (Sutton, 1988) to update the critic, which implicitly assumes that actions are selected based on each perceived state, rather than a sequence of actions predicted at the start of the episode, as in ERL approaches. In this paper, we address this limitation by predicting the N-step return (Sutton & Barto, 2018) for a sequence of actions using a Transformer architecture, enabling the learning of sequence values within an off-policy framework.

**Transformer in RL.** Over the past few years, the Transformer architecture (Vaswani, 2017) has emerged as one of the most powerful models for sequence data. It has been integrated into RL across various domains, capitalizing on their strengths in sequence pattern recognition from static datasets and functioning as a memory-based architecture, which aids in task understanding and credit assignment. Applications of Transformers in RL include offline RL (Chebotar et al., 2023; Yamagata et al., 2023; Wu et al., 2024), offline-to-online fine-tuning (Zheng et al., 2022; Ma & Li, 2024; Zhang et al., 2023), handling partially observable states (Parisotto et al., 2020; Ni et al., 2024; Lu et al., 2024), and model-based RL (Lin et al., 2023). However, the use of Transformers within a model-free online RL framework, specifically for sequence action prediction and evaluation, remains largely unexplored (Yuan et al., 2024). This is noteworthy, as similar techniques, such as action chunking (Bharadhwaj et al., 2024), have already proven successful in other domains like imitation learning.

In this paper, we propose **Transformer-based Off-Policy ERL (TOP-ERL)**, which leverages the Transformer as a critic to predict the value of action sequences. Given a trajectory from ERL, we split it into smaller segments and input them into the Transformer for value prediction. We adapt off-policy update rules for action sequences, using the N-step TD error for critic updates. The policy then selects action sequences based on the preferences of the Transformer critic, similar to SAC. Compared to existing ERL and SRL methods, we show that TOP-ERL improves both policy quality and sample efficiency, outperforming them in several simulated robot manipulation tasks.

**Our contributions** are: (a) A novel off-policy RL method that integrates the Transformer as a critic for action sequences in a model-free, online RL framework. (b) The use of N-step return as the learning objective for the Transformer critic. (c) Comprehensive evaluation on simulated robotic manipulation tasks, demonstrating superior performance against baselines. (d) Analysis of different critic update rules, design choices, and the impact of segment length on model performance.

## 2 RELATED WORKS

**Episodic RL.** The study of ERL approaches dates back to the 1990s. Early approaches employed black-box optimization techniques to update parameters of policies, such as small MLPs (Whitley et al., 1993; Igel, 2003; Gomez et al., 2008). Due to the substantial data requirements of black-box algorithms and the limited computational resources available at the time, these approaches were constrained to low-dimensional tasks like Pendulum and Cart Pole. Subsequent works (Salimans et al., 2017; Mania et al., 2018) demonstrated that, given sufficient computational resources, ERL methods can also achieve comparable performance to step-based RL on challenge locomotion tasks, such as Ant and Humanoid, at the cost of more samples for convergence. Another line of research in ERL focuses on more compact policy representations. Peters & Schaal (2008) first proposed using movement primitives (MPs) as parameterized policies for ERL, reducing the search space from the high-dimensional neural network parameter space to the MP weight space, which typically ranges from 20 to 50 dimensions, resulting in less samples required for convergence. Using MPs as policies also provides additional benefits, such as smooth trajectory generation and more consistent exploration (Li et al., 2024). MP-based ERL approaches have demonstrated the ability to master complex manipulation tasks such as robot baseball (Peters & Schaal, 2008) and juggling (Ploeger et al., 2021). To further improve sample efficiency, Abdolmaleki et al. (2015) introduced a model-based method to enable more sample-efficient black-box searching. However, these methods are limited in handling tasks with contextual variations, e.g., changing goals. To address this limitation, Abdolmaleki et al. (2017) and Celik et al. (2022) extend MP-based ERL by using linear policies conditioned on context. Otto et al. (2022) enhanced contextual MPRL by employing neural network policies and trust-region regularized policy update. Despite these advances, existing ERL methods generally treat the episodic trajectory as a black box. While this approach allows them to handle sparse and even non-Markovian rewards, ignoring the temporal structure within each episode leads

to lower sample efficiency compared to step-based methods, especially in settings with dense rewards. To address this issue, a most recently proposed method, *Temporally-Correlated ERL* (TCE) (Li et al., 2024) introduced a more efficient update scheme that "opens the black-box" and utilizes sub-segment information for policy update while retaining the benefit of episodic exploration. Although TCE improves the sample efficiency of contextual ERL methods, it still relies on on-policy policy gradient updates, which are considered sample-inefficient. To the best of our knowledge, TOP-ERL is the first off-policy ERL algorithm capable of handling contextual tasks.

**Transformers in model-free RL.** Inspired by the success of Transformers in domains requiring sequence reasoning, the study incorporating Transformers in RL to solve tasks that require long-horizon memory emerged. However, using standard Transformers in RL could result in performance comparable to random policy (Parisotto et al., 2020). To address this issue, *Gated Transformer-XL* (GTrXL) (Parisotto et al., 2020) augmented Transformer-XL with GRU-style gating layers between multi-head self-attention layers, stabilizing the training of deep Transformer networks (up to 12 layers) with online RL. Another research line focuses on utilizing Transformers to enhance offline RL, where the learning process is based on a fixed dataset collected by arbitrary behavior policies. *Decision Transformers* (Chen et al., 2021) were the first to formulate offline RL as a sequence modeling problem. Subsequent works extended this approach by incorporating dynamic history length adjustment (Wu et al., 2024), Q-learning (Yamagata et al., 2023), and replacing the Transformer with a more efficient state-space model (Ota, 2024). Online Decision Transformers (Zheng et al., 2022) further advanced Decision Transformer by introducing online fine-tuning. In contrast to these studies, which primarily focus on offline RL or fine-tuning pre-trained models, TOP-ERL is designed for online RL and does not rely on offline training. Additionally, TOP-ERL is not designed to solve tasks that require long-horizon memory. Instead, it focuses on using a Transformer-based critic to improve multi-step TD learning within the ERL framework.

### 3 PRELIMINARIES

#### 3.1 OFF-POLICY REINFORCEMENT LEARNING

**Markov decision process (MDP).** RL learns policies that maximize cumulative rewards in a given environment, modeled as an MDP. Formally, we consider an MDP defined by a tuple  $(\mathcal{S}, \mathcal{A}, P, r, \gamma)$ , where both state  $\mathcal{S}$  and action spaces  $\mathcal{A}$  are continuous. Here,  $P(s'|s, a)$  denotes the state transition probability,  $r(s, a)$  is the reward function, and  $\gamma \in [0, 1]$  is the discount factor. The goal of RL is to find a policy  $\pi(a|s)$  that maximizes the expected *return*, which is the sum of discounted future rewards as  $G_t(s_t, a_t) = \sum_{i=0}^{\infty} \gamma^i r_{t+i}$ .

In **off-policy RL**, the agent learns a policy  $\pi(a|s)$  using data generated by a different behavior policy  $\pi_b(a|s)$ . This enables off-policy methods to reuse past experiences, significantly improving sample efficiency against on-policy methods. A common approach in off-policy RL is to use a *critic*, which estimates the action-value function  $Q^\pi(s, a)$  and is updated using a temporal difference (TD) error

$$Q^\pi(s, a) = \mathbb{E}_\pi[G_t | s_t = s, a_t = a], \quad \delta_t = r_t + \gamma Q^\pi(s_{t+1}, a_{t+1}) - Q^\pi(s_t, a_t), \quad (1)$$

where the TD error  $\delta_t$  estimates the difference between the current Q-value and the target Q-value. While the above single-step TD error is useful, it can suffer from high bias and slow convergence, especially in environments with delayed rewards. To address this, N-step returns (Sutton, 1988) are often used to provide a better balance between bias and variance.

**The N-step return** extends the single-step TD return by incorporating multiple future time-steps into the target. Unlike bootstrapping after a single time step, the N-step return accumulates rewards over  $N$  steps before using the current value estimate for bootstrapping. These estimates are typically less biased than the 1-step return, but also contain more variance. In off-policy settings, the N-step return typically involves importance sampling (Sutton & Barto, 2018), as the selection of the future action path used to accumulate rewards differs from the current policy  $\pi(a|s)$ , seen as:

$$G_t^{(N)}(s_t, a_t) = \sum_{i=0}^{N-1} \left( \prod_{j=0}^i \rho_{t+j} \right) \gamma^i r_{t+i} + \left( \prod_{j=0}^{N-1} \rho_{t+j} \right) \gamma^N Q^\pi(s_{t+N}, a_{t+N}), \quad (2)$$

where  $\rho_t = \frac{\pi(a_t|s_t)}{\pi_b(a_t|s_t)}$  is the importance sampling ratio, ensuring that updates remain unbiased even when using trajectories generated by a different policy.

162 Despite this mathematical correction, applying N-step returns in off-policy learning can face dif-  
 163 ficulties, particularly for long sequences. The product of importance ratios can become highly  
 164 volatile, leading to either exploding or vanishing values over extended trajectories, which in turn  
 165 can cause high variance in the value estimates and destabilize the learning process. In TOP-ERL,  
 166 however, we employ N-step return for computing the target value of a sequence of actions, i. e.  
 167  $G_t^{(N)}(s_t, a_t, a_{t+1}, \dots, a_{t+N})$ , where N-step actions are determined in a sequence read from the re-  
 168 play buffer, rather than sampled from the policy. Therefore, the resulting formulation does not  
 169 contain the importance weights. We will further discuss the details in Sec. 4.3.

### 171 3.2 EPISODIC REINFORCEMENT LEARNING (ERL)

172 **Episodic RL** (Whitley et al., 1993; Kober & Peters, 2008) focuses on predicting an entire sequence  
 173 of actions to complete a task, optimizing the cumulative return without explicitly considering de-  
 174 tailed state transitions within the episode. Typically, ERL methods utilize a parameterized trajectory  
 175 generator, such as motion primitives (MP) (Schaal, 2006; Paraschos et al., 2013), which predicts a  
 176 trajectory parameter vector  $\mathbf{w}$ . This vector is then mapped to a full action trajectory  $\mathbf{a}(\mathbf{w}) = [\mathbf{a}_t]_{t=0}$ ,  
 177 where  $T$  is the trajectory length. Here,  $\mathbf{a}_t \in \mathbb{R}^D$  denotes the action at time step  $t$ , and  $D$  represents  
 178 the dimensionality of the action space, such as the degrees of freedom (DOF) in a robotic system.  
 179 In this framework, an intelligent agent—such as a robot—executes the predicted action sequence  
 180 directly as motor commands or follows the trajectory using a tracking controller.

181 Although ERL predicts an entire action trajectory, it still adheres to the *Markov property*, where  
 182 the state transition probability depends only on the current state and action (Sutton & Barto, 2018).  
 183 Thus, while the action sequence in ERL spans multiple time steps, the underlying process remains  
 184 consistent with the MDP formalism. This approach is conceptually related to techniques such as  
 185 action repeat (Braylan et al., 2015) and temporally correlated action selection (Raffin et al., 2022;  
 186 Eberhard et al., 2022), which also incorporate temporal dependencies into action selection.

187 **Movement Primitives (MP)**, as parameterized trajectory generators, play a crucial role in ERL. We  
 188 briefly highlight key MP methodologies and their mathematical foundations used in this work, with  
 189 a more detailed discussion in Appendix B. Schaal (2006) introduced Dynamic Movement Primitives  
 190 (DMPs), which incorporates a forcing term into a dynamical system to generate smooth trajectories  
 191 from a given initial condition, such as a robot’s position and velocity at a particular time<sup>1</sup>.

$$192 \tau^2 \ddot{y} = \alpha(\beta(g - y) - \tau \dot{y}) + f(x), \quad f(x) = x \frac{\sum \varphi_i(x) w_i}{\sum \varphi_i(x)} = x \boldsymbol{\varphi}_x^\top \mathbf{w}, \quad (3)$$

195 where  $y = y(t)$ ,  $\dot{y} = dy/dt$ ,  $\ddot{y} = d^2y/dt^2$  denote the position, velocity, and acceleration of the  
 196 system at time  $t$ , respectively. Constants  $\alpha$  and  $\beta$  are spring-damper parameters, with  $g$  as the goal  
 197 attractor and  $\tau$  as a time constant modulating the speed of trajectory execution. The functions  $\varphi_i(x)$   
 198 represents the basis functions for the forcing term, and the trajectory’s shape is determined by the  
 199 weight parameters  $w_i \in \mathbf{w}$ , for  $i = 1, \dots, N$ . The trajectory  $[y_t]_{t=0:T}$  is typically computed by nu-  
 200 merically integrating the dynamical system from the start to the end. Building on the same concepts,  
 201 Li et al. (2023) proposed Probabilistic Dynamic Movement Primitives (ProDMPs), which directly  
 202 uses the closed-form solution of Eq.(3). ProDMP employs a linear basis function representation to  
 203 directly map a parameter vector  $\mathbf{w}$  to its corresponding trajectory  $[y_t]_{t=0:T}$ :

$$204 y(t) = \boldsymbol{\Phi}(t)^\top \mathbf{w} + c_1 y_1(t) + c_2 y_2(t). \quad (4)$$

205 Here, the terms  $c_1 y_1(t) + c_2 y_2(t)$  ensure precise trajectory initialization, with the constants  $c_1, c_2$   
 206 calculated based on the initial condition  $y_b, \dot{y}_b$  at time  $t_b$ . The term  $\boldsymbol{\Phi}(t)$  denotes the integral form  
 207 of the basis functions  $\varphi$  used in the Eq.(3). Unlike DMP, ProDMP benefits from the closed-form  
 208 solution of the dynamic system, enabling faster computation and probabilistic modeling without the  
 209 burden for numerical integration. This allows for flexible trajectory generation and precise initial  
 210 condition enforcement. In TOP-ERL, we leverage ProDMP’s fast initial condition enforcement to  
 211 compute accurate target values for the Transformer critic, thereby reducing bias in policy learning.

212 **ERL Learning Objectives.** A key distinction between ERL and step-based RL (SRL) lies in the  
 213 action space. ERL shifts the solution search from the per-step action space  $\mathcal{A}$  to a parameterized  
 214

215 <sup>1</sup>An initial condition in mathematics refers to the value of a function or its derivatives at a starting point,  
 which can be specified at any time and is not necessarily at  $t = 0$ .

trajectory space  $\mathcal{W}$ , predicting the trajectory parameters as  $\pi(\mathbf{w}|\mathbf{s})$ . As a result, a trajectory parameterized by  $\mathbf{w}$  is treated as a single data point in  $\mathcal{W}$ . This often leads ERL to employ black-box optimization methods for trajectory optimization (Salimans et al., 2017). The learning objective in ERL is often formulated using an importance sampling ratio, such as in BBRL (Otto et al., 2022)

$$\text{Update using trajectory parameter: } J = \mathbb{E}_{\pi_{\text{old}}(\mathbf{w}|\mathbf{s})} \left[ \frac{\pi_{\text{new}}(\mathbf{w}|\mathbf{s})}{\pi_{\text{old}}(\mathbf{w}|\mathbf{s})} G^{\pi_{\text{old}}}(\mathbf{s}, \mathbf{w}) \right], \quad (5)$$

where  $\pi$  represents the policy parameterized by  $\theta$ , typically using a neural network. The terms *new* and *old* refer to the current policy being optimized and the policy used for data collection, respectively. The initial state  $\mathbf{s} \in \mathcal{S}$  defines the starting configuration and objective of the task, serving as input to the policy. The policy  $\pi_{\theta}(\mathbf{w}|\mathbf{s})$  determines the likelihood of selecting trajectory parameters  $\mathbf{w}$ . The term  $G^{\pi_{\text{old}}}(\mathbf{s}, \mathbf{w}) = \sum_{t=0}^T \gamma^t r_t$  represents the return accumulated by executing the trajectory under an old policy, where  $\gamma$  is the discount factor and  $r_t$  is the reward at time step  $t$ . By leveraging parameterized trajectory generators like MPs, ERL benefits from consistent exploration, smooth action trajectories, and improved robustness against local optima, as highlighted by Otto et al. (2022). To further enhance learning efficiency, recent work TCE (Li et al., 2024) proposes a hybrid update strategy that decomposes the trajectory parameter-wise update into the segment-wise updates, incorporating per-step information into ERL’s learning objective. This approach divides the longer action trajectory into smaller segments, calculating the return of each segment. The new learning objective adapts Eq.(5), with the maximization of segment-wise returns as

$$\text{Update using segments: } J = \mathbb{E}_{\pi_{\text{old}}(\mathbf{w}|\mathbf{s})} \left[ \frac{1}{K} \sum_{k=1}^K \frac{p^{\pi_{\text{new}}}([\mathbf{a}_t^k]_{t=0:L}|\mathbf{s})}{p^{\pi_{\text{old}}}([\mathbf{a}_t^k]_{t=0:L}|\mathbf{s})} G^{\pi_{\text{old}}}(\mathbf{s}_0^k, [\mathbf{a}_t^k]_{t=0:L}) \right], \quad (6)$$

where  $K$  and  $L$  represent the number and length of the trajectory segments, respectively, with  $K = 25$  in the original paper and  $k = 1, \dots, K$  denotes the segment index. In this expression,  $p^{\pi}$  denotes the likelihood of reproducing the segment, calculated using the parameterized policy  $\pi_{\theta}(\mathbf{w}|\mathbf{s})$ , and  $G(\mathbf{s}_0^k, [\mathbf{a}_t^k]_{t=0:L})$  represents the return of executing the  $k$ -th action sequence segment  $[\mathbf{a}_t^k]_{t=0:L}$  from the segment’s starting state  $\mathbf{s}_0^k$ . It is worth noting, despite the usage of importance sampling, both Eq. (5) and Eq. (6) still remain within the on-policy RL framework. In TOP-ERL, we employ a similar strategy in splitting a long action trajectory into smaller segments, and use these segments for efficient critic and policy updates, under an off-policy framework.

## 4 TRANSFORMER-BASED OFF-POLICY ERL

In this section, we present TOP-ERL, an innovative off-policy solution for ERL that leverages a Transformer for action sequence evaluation. The section is structured as follows: Section 4.1 introduces the Gaussian policy modeling and action trajectory generation, followed by the design of the transformer critic in Section 4.2. The learning objectives for the critic and policy are detailed in Section 4.3 and Section 4.4, respectively, with additional technical details. Lastly, we summarize other design choices in Section 4.5. [The main contributions of our model are described from Section 4.2 to Section 4.4, while the remaining sections cover techniques adopted from the literature.](#)

### 4.1 TRAJECTORY GENERATION: TECHNIQUES ADOPTED FROM ERL LITERATURE

TOP-ERL adopts a policy structure similar to previous ERL approaches, such as BBRL (Otto et al., 2022). As shown in Fig. 1, our policy is modeled as a Gaussian distribution,  $\pi_{\theta}(\mathbf{w}|\mathbf{s}) = \mathcal{N}(\mathbf{w}|\boldsymbol{\mu}_{\mathbf{w}}, \boldsymbol{\Sigma}_{\mathbf{w}})$ , where  $\mathbf{s}$  defines the initial observation and the task objective, and  $\mathbf{w}$  represents the parameters of the movement primitive (MPs). In TOP-ERL, we employ ProDMPs (Li et al., 2023) to help correct the target computation via enforcing the initial condition of the MP, as discussed later in Section 4.3.1. Given an initial task state  $\mathbf{s}$ , the policy predicts the Gaussian parameters and samples a parameter vector  $\mathbf{w}^*$ . This vector is then passed into the movement primitive to generate the action trajectory  $[\mathbf{a}_t]_{t=0:T}$ . The agent then executes the action trajectory in the environment until the end of the episode. During the rollout, both the state trajectory and the reward trajectory are recorded. These, along with the action trajectory, are subsequently stored in the replay buffer  $\mathcal{B}$  for later use.

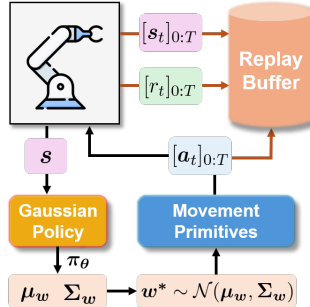


Figure 1: Trajectory generation and environment rollout.

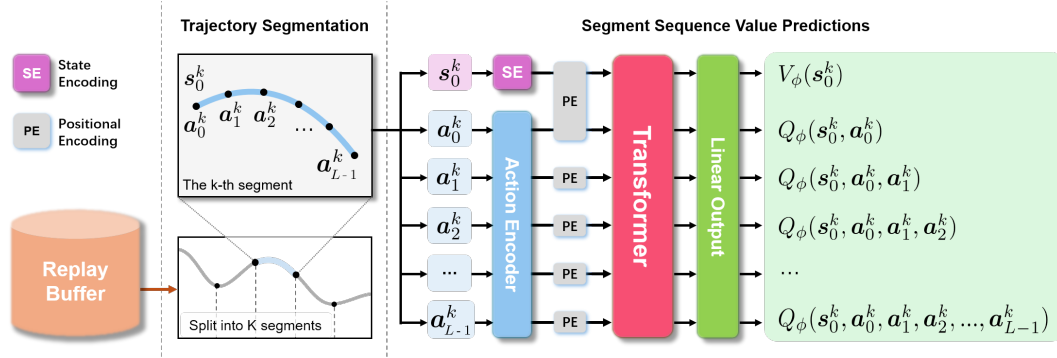


Figure 2: Architecture overview of the Transformer critic, as described in Sec. 4.2.

#### 4.2 TRANSFORMERS AS VALUE PREDICTOR FOR ACTION SEQUENCES

An architectural overview of our Transformer critic is depicted in Fig. 2. At each iteration, we sample a batch  $B$  of trajectories from the replay buffer and split each trajectory into  $K$  segments, where each segment is  $L$  time steps long. An ablation on how to select the segment length  $L$  can be found in Sec. 5.3. The transformer-based critic has  $L + 1$  input tokens that are given by each action in the segment  $\{a_t^k\}_{t=0:L-1}$  and the starting state  $s_0^k$  of the corresponding segment. These tokens are first processed by corresponding state and action encoders, each modeled by a single linear layer. Positional information is added to the processed tokens through a trainable positional encoding, with  $s_0^k$  and the first action token  $a_0^k$  sharing the same positional encoding (both at  $t = 0$ ). The tokens are subsequently fed into a decoder-only Transformer, followed by a linear output layer, producing  $L + 1$  output tokens. The first output represents the state value  $V_\phi(s_0^k)$  for the starting state, while the remaining outputs correspond to the state-action values for the subsequent action sequence. For example,  $Q_\phi(s_0^k, a_0^k, a_1^k, a_2^k)$  represents the value of executing the actions  $a_0^k, a_1^k, a_2^k$  sequentially from the starting state  $s_0^k$  and subsequently following policy  $\pi$ . A causal mask is applied in the Transformer to ensure that actions do not attend to future steps.

#### 4.3 N-STEP RETURNS AS THE TARGET FOR TRANSFORMER CRITIC

For each predicted state-action value  $Q(s_0, a_0^k, \dots, a_{N-1}^k)$  we utilize the N-step return as its target. The objective to update the parameters  $\phi$  of the critic is the N-step squared TD error<sup>2</sup>

$$\begin{aligned} \text{Critic loss: } \mathcal{L}(\phi) = & \frac{1}{L} \sum_{N=1}^{L-1} \left[ \underbrace{Q_\phi(s_0^k, a_0^k, \dots, a_{N-1}^k)}_{\text{Predicted value of N actions}} - \underbrace{G^{(N)}(s_0^k, a_0^k, \dots, a_{N-1}^k)}_{\text{Target using N-step return}} \right]^2 \\ & + \left[ \underbrace{V_\phi(s_0^k)}_{\text{Predicted state value}} - \underbrace{\mathbb{E}_{\tilde{w} \sim \pi_\theta(\cdot|s)} [Q_{\phi_{\text{tar}}}(s_0^k, \tilde{a}_0^k, \dots, \tilde{a}_{L-1}^k)]}_{\text{Target of new actions using } \tilde{w}} \right]^2, \quad (7) \end{aligned}$$

$$\text{N-step return: } G^{(N)}(s_0^k, a_0^k, \dots, a_{N-1}^k) = \underbrace{\sum_{i=0}^{N-1} \gamma^i r_i}_{\text{N-step rewards}} + \underbrace{\gamma^N V_{\phi_{\text{tar}}}(s_N)}_{\text{Future return after N-step}}. \quad (8)$$

Here,  $N \in [1, L - 1]$  represents the number of actions in a sub-sequence starting from  $s_0^k$ . The term  $Q_{\phi_{\text{tar}}}(s_0^k, \tilde{a}_0^k, \dots, \tilde{a}_{L-1}^k)$  in Eq.(7) denotes the target value of  $V_\phi(s_0^k)$  with actions  $\tilde{a}_0^k, \dots, \tilde{a}_{L-1}^k$  generated by new MP parameters  $\tilde{w}$  sampled from the current policy,  $\tilde{w} \sim \pi_\theta(\cdot | s)$ . The term  $V_{\phi_{\text{tar}}}(s_N)$  in Eq.(8) represents the future return after  $N$  steps. Both  $Q_{\phi_{\text{tar}}}$  and  $V_{\phi_{\text{tar}}}$  are predicted by a target critic (Mnih et al., 2015), with a delayed update rate  $\rho = 0.005$ . Please note that  $Q_{\phi_{\text{tar}}}$  and  $V_{\phi_{\text{tar}}}$  are the same transformer network, with and without action tokens.

<sup>2</sup>For simplicity, we omit the expectation over buffer  $B$  and average over segment number  $K$  in Eq.(7).

In off-policy RL literature, there are several alternatives to replace  $V_{\phi_{\text{tar}}}(\mathbf{s}_N)$  in Eq.(8). However, we find that this choice alone performs well in our experiments. In other words, TOP-ERL does not necessarily rely on some common off-policy techniques, such as the clipped double-Q (Fujimoto et al., 2018), to be stable and effective. We attribute this to the usage of the N-step returns, which help reduce value estimation bias. In Sec. 5.3, we show that our model can be further improved using these augmentations, though at a cost of additional computation.

Unlike Eq.(2), our N-step return targets  $G^{(N)}(\mathbf{s}_0^k, \mathbf{a}_0^k, \dots, \mathbf{a}_{N-1}^k)$  in Eq.(8) do not include importance sampling as the the action sequence  $\mathbf{a}_0^k, \dots, \mathbf{a}_{N-1}^k$  is directly used as input tokens for the Q-function. Hence, the actions are fixed and we do not require to compute any expectations over the current policy’s action selection. Hence, using the fixed action sequence in Eq.(8) as input to the Q-Function eliminates the need for importance sampling, thus avoiding the high variance typically introduced by it in off-policy methods, as discussed in Sec. 3.1.

#### 4.3.1 ENFORCE INITIAL CONDITION FOR NEWLY PREDICTED ACTION SEQUENCE

When calculating the target value  $Q_{\phi_{\text{tar}}}(\mathbf{s}_0^k, \tilde{\mathbf{a}}_0^k, \dots, \tilde{\mathbf{a}}_{L-1}^k)$  in Eq.(7), a new parameter vector is sampled from the current policy  $\tilde{\mathbf{w}} \sim \pi_{\theta}(\cdot | \mathbf{s})$ , generating a new action trajectory  $[\tilde{\mathbf{a}}_t^k]_{t=0:T}$ , with  $[\tilde{\mathbf{a}}_t^k(\tilde{\mathbf{w}})]_{t=0:L-1}$  as a sub-sequence. However, this sequence is not necessarily guaranteed to pass through the segment’s starting state  $\mathbf{s}_0^k$ , which creates a mismatch between the state and corresponding action sequence when querying the target in Eq.(7). To address this issue, we append the old reference position to  $\mathbf{s}_0^k$ , and then leverage the dynamic system formulation inherent in ProDMPs by setting the initial condition of the new action sequence to match the old reference at  $\mathbf{s}_0^k$ , as illustrated in Fig. 3. The resulting action sequence  $[\tilde{\mathbf{a}}_t^k(\tilde{\mathbf{w}}, \mathbf{s}_0^k)]_{t=0:L-1}$  is therefore depending on both the MP parameters  $\tilde{\mathbf{w}}_{\theta}(\mathbf{s})$  and the initial condition  $\mathbf{s}_0^k$ . This approach is mathematically equivalent to resetting the initial conditions of an ordinary differential equation (ODE), ensuring consistency between the state and action sequences. Further mathematical details are provided in Appendix B.3.

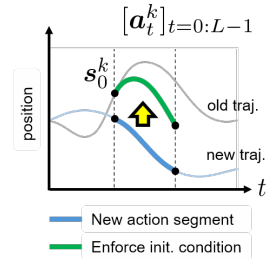


Figure 3: Enforce action initial condition

#### 4.4 POLICY UPDATES USING THE TRANSFORMER CRITIC

We utilize the transformer critic to guide the training of our policy, using the reparameterization trick similar to that introduced by SAC (Haarnoja et al., 2018a). The learning objective is to maximize the expected value of the averaged action sequence over varying lengths, defined as:

$$\text{Policy Objective: } J(\theta) = \mathbb{E}_{\mathbf{s} \sim B} \mathbb{E}_{\tilde{\mathbf{w}} \sim \pi_{\theta}(\cdot | \mathbf{s})} \left[ \frac{1}{KL} \sum_{k=1}^K \sum_{N=0}^{L-1} Q_{\phi}(\mathbf{s}_0^k, [\tilde{\mathbf{a}}_t^k]_{t=0:N}) \right], \quad (9)$$

where  $[\tilde{\mathbf{a}}_t^k]_{t=0:N} = [\tilde{\mathbf{a}}_t^k(\tilde{\mathbf{w}}_{\theta}, \mathbf{s}_0^k)]_{t=0:N}$  denotes the new action sequence generated by the new MP parameters  $\tilde{\mathbf{w}}_{\theta} \sim \pi_{\theta}(\cdot | \mathbf{s})$ . To ensure consistency between the initial state  $\mathbf{s}_0^k$  and the new action sequence, we apply the same initial condition enforcement technique discussed in Section 4.3.1. This learning objective allows the policy  $\pi_{\theta}(\mathbf{w} | \mathbf{s})$  to be trained based on the *value preferences* provided by the Transformer critic.

#### 4.5 ADDITIONAL DESIGN CHOICES FROM THE LITERATURE FOR STABLE LEARNING

We summarize the key learning steps in Algorithm1. To effectively capture a broader range of correlations in both temporal and DoF movements, we utilize a full covariance matrix  $\Sigma_{\mathbf{w}}$  in the Gaussian policy (Li et al., 2024). Since the Gaussian policy over MP parameters is typically high-dimensional, we employ the Trust Region Projection Layer (TRPL) (Otto et al., 2021) for stable policy updates, following the design of previous ERL methods (Otto et al., 2022; Li et al., 2024; Celik et al., 2024). For the Transformer critic, we apply Layer Normalization (Ba, 2016) as the sole data normalization technique, while disabling dropout, as we found it detrimental to performance. In our experiments, we identified the segment length  $L$  as a key hyperparameter. The best results were achieved by randomly sampling  $L$  at each update iteration, which we attribute to the Transformer critic’s ability to attend to different time horizons, resulting in more robust outcomes.

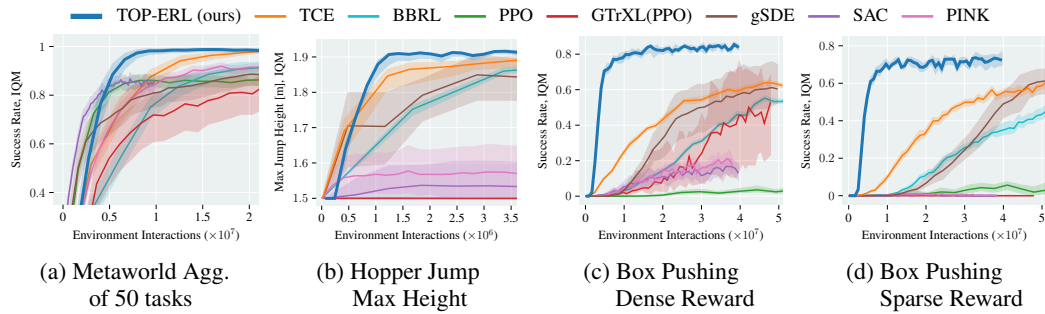


Figure 4: Task Evaluation of (a) Metaworld success rate of 50 tasks aggregation. (b) Hopper Jump Max Height. (c) Box Pushing success rate in dense reward, and (d) sparse reward settings.

## 5 EXPERIMENTS

Our experiments are designed to address the following questions: I) Can TOP-ERL improve sample efficiency in classical ERL tasks characterized by challenging exploration problems? II) How does TOP-ERL perform in large-scale, general manipulation benchmarks? III) How do key design choices affect the performance of TOP-ERL? We compare TOP-ERL against a set of strong baselines. For the ERL comparisons, we select **BBRL** and **TCE** as SoTA ERL methods. For step-based RL, we use **PPO** (on-policy) and **SAC** (off-policy) as established baselines. Additionally, we employed **gSDE** and **PINK**, two step-based RL methods that augment with consistent exploration techniques, to test the impact of exploration strategies. To assess the impact of using Transformer-based architectures in RL, we include **GTrXL** as baseline for online RL with Transformers architecture. It is worth noting that in the original work, GTrXL was trained using VMPO. However, since the original code was not open-sourced, we used the implementation from Liang et al. (2018), where GTrXL is trained with PPO instead. For all ERLs, the trajectories are generated using ProDMPs with the same hyperparameters and tracked with PD-controllers (or P-controller for MetaWorlds); for all the SRLs, the action outputs are torque (or delta position for MetaWorlds). An overview of the baselines can be found in Table 3, and details regarding the implementation and hyperparameters are provided in the Appendix E.

The evaluation of TOP-ERL are structured in three phases. First, we demonstrated that TOP-ERL significantly improve the sample efficiency over state-of-the-art ERL methods, showcasing its ability to better handle the challenges of sparse rewards and difficult exploration scenarios (Li et al., 2024). Next, we evaluate TOP-ERL on the Meta-World MT50 (Yu et al., 2020) benchmark, a large-scale suite of general manipulation tasks. In this setting, TOP-ERL consistently outperform all baselines, demonstrated TOP-ERL’s ability to generalize across a wide range of manipulation tasks. Finally, we conduct a comprehensive ablation study to analysis which ingredient accounts for the strong performance of TOP-ERL. The results confirm that these components are essential to achieving the strong performance observed with TOP-ERL. To ensure a robust evaluation, all **empirical** results are reported using Interquartile Mean (IQM), accompanied by a 95% stratified bootstrap confidence interval (Agarwal et al., 2021) across 8 random seeds.

### 5.1 IMPROVING SAMPLE EFFICIENCY IN TASKS WITH CHALLENGING EXPLORATION

ERL methods are renowned for their superior exploration abilities, which often give them an advantage over step-based methods in environments with exploration challenges. However, ERL

---

#### Algorithm 1 TOP-ERL

---

- 1: Initialize critic  $\phi$ ; target critic  $\phi_{tar} \leftarrow \phi$
  - 2: Initialize policy  $\theta$  and replay buffer  $\mathcal{B}$
  - 3: **repeat**
  - 4:   Reset environment and get initial task state  $\mathbf{s}$
  - 5:   Predict the policy mean  $\mu_w$  and covariance  $\Sigma_w$
  - 6:   Sample  $w^*$  and generate action trajectory  $[\mathbf{a}]_{0:T}$
  - 7:   Execute the action trajectory till task ends.
  - 8:   Store the visited states  $[\mathbf{s}]_{0:T}$ , rewards  $[r]_{0:T}$ , and the action  $[\mathbf{a}]_{0:T}$  trajectories in replay buffer  $\mathcal{B}$
  - 9:   **for** each update step **do**
  - 10:     From  $\mathcal{B}$ , sample a batch of  $\mathbf{s}, \mathbf{a}, r$  trajectories.
  - 11:     Split them into  $K$  segments, each  $L$  time steps.
  - 12:     Compute N-step return targets as in Eq.(8)
  - 13:     Update transformer critic, using Eq.(7)
  - 14:     Update policy, using Eq.(9)
  - 15:   **end for**
  - 16:   Update target critic  $\phi_{tar} \leftarrow (1 - \rho) \phi_{tar} + \rho \phi$
  - 17: **until** converged
-

algorithms are also notoriously sample inefficient, limiting their applicability in scenarios where obtaining samples is expensive. In this evaluation, we investigate whether TOP-ERL can address this limitation by comparing it with baselines on three challenging tasks from Li et al. (2024) and Otto et al.: HopperJump, a sparse-reward environment where the objective is to maximize the jump height within an episode, and two variants of a contact-rich Box Pushing task. We evaluate the Box Pushing task under both dense and sparse reward settings. Further details about the environments and rewards can be found in Appendix C. The results of these experiments, shown in Fig. 4, demonstrate that TOP-ERL achieved the highest final performance across all three tasks. **Notably**, in the dense-reward Box Pushing task, TOP-ERL reached an 80% success rate after just 10 million samples, while the second-best method, TCE, only reaches 60% success after 50 million samples. Similar results is observed in the sparse-reward Box Pushing task, where TOP-ERL reaches 70% success rate with 14 million environment interactions, while TCE and gSDE require 50 million samples to reach 60% success. GTrXL performs moderately in the dense-reward setting, achieving a 50% success rate, but fails completely in the sparse-reward environment. Step-based methods like SAC, PINK and PPO failed in both cases, underscoring the difficulty of these tasks. Among the step-based algorithms, only gSDE achieved comparable performance in compare with ERL methods in these three environments, which we attribute to its state-dependent exploration strategy.

## 5.2 CONSISTENT PERFORMANCE IN LARGE-SCALE MANIPULATION BENCHMARKS

In the previous evaluation, we demonstrated that TOP-ERL significantly improves sample efficiency compared to state-of-the-art ERL baselines, while maintaining strong performance in tasks with challenge exploration. In this evaluation, we focus on answering the second question: How does TOP-ERL perform on standard manipulation benchmarks with dense rewards? We conducted experiments on the Meta-World benchmark (Yu et al., 2020), reporting the aggregated success rate **across 50 tasks** in the MT50 task set. To ensure a fair comparison, we followed the same evaluation protocol described in Otto et al. (2022) and Li et al. (2024), where an episode is only considered successful if the success criterion is met at the end of the episode, a more rigours measure than the original setting where success at any time step counts. The results in Fig. 4a show that TOP-ERL achieved highest asymptotic success rate (98%) after 10 million samples. TCE was able to achieve the same success rate but required 20 million interactions. SAC also converged after 10 million samples but with a significantly lower success rate of 85%. BBRL and other step-based methods achieved moderate success rate but required significantly more samples.

## 5.3 ABLATION STUDY AND DISCUSSION

**Single Q-Network leads to stable and efficient training.** We compare four common design choices for targets calculation in Q-function update in Eq.(8): 1) V-Target which uses a single V target network, 2) Q-Target, which employs single Q target network, 3)V-Ensemble, which consists of an ensemble of predictions from two V target networks, 4) V-Clip, which takes the minimum of two V target networks. Detailed description of these target calculation approaches can be found in Appendix A. Fig. 5 presents the learning curves for TOP-ERL in dense-reward (5a) and **sparse**-reward (5b) Box Pushing, while Table 1 presents the numerical success rate and computation times per update. The results demonstrate that using a single V target network yields performance comparable to approaches that rely on two target networks, with additionally benefit of significantly reduced computation time (approximately 50% faster). We attribute the stable performance with single target network to the use of N-step Bellman equation in target calculation, as discussed in Sec. 4.3.

**Key Components Ablation.** We evaluate the impact of five key components on the performance of TOP-ERL: trust region constraints in policy updates, enforcing the initial condition at each segment, the presence of layer normalization, fixed vs. random segment lengths, and the inclusion of dropout in Transformer layers. These evaluations were conducted in both dense-reward and sparse-reward Box Pushing environments using 8 random seeds. The results, presented in Fig. 5 as dashed lines, show performance for TOP-ERL with corresponding component been added or removed. The results indicate that the random segment length has the most significant effect on TOP-ERL’s performance. When using fixed 25 segments the success rate dropped from 80% to 35% in the dense-reward setting, and from 70% to 20% in the sparse-reward setting. Layer normalization, trust region constraints, and enforcing initial conditions also contributed positively to the performance. Interestingly, adding even a small dropout rate (0.05 in the ablation) had negative impacts on the performance in

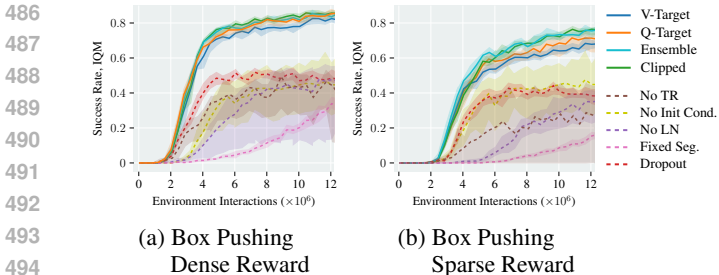


Figure 5: Performance of different critic update strategies (solid lines) and model ablations (dashed lines), using Box pushing dense and sparse reward settings respectively.

Table 1: Quantitative performance and update time of different critic update strategies. With additional computational cost, TOP-ERL can be further enhanced.

| Variant            | # critic | Time s / iter ↓ | Dense Success, % ↑ | Sparse Success, % ↑ |
|--------------------|----------|-----------------|--------------------|---------------------|
| V-Target (default) | 1        | 1.55            | 82.0±2.6           | 65.7±4.0            |
| Q-Target           | 1        | 2.44            | 86.1 ± 2.7         | 69.1 ± 7.5          |
| V-Ensem.           | 2        | 2.49            | 83.8 ± 3.1         | 75.7 ± 4.4          |
| V-Clip             | 2        | 2.49            | 86.0 ± 3.2         | 75.5 ± 3.7          |

both tasks. We hypothesize that this effect may be attributed to the use of a relatively small replay buffer combined with a higher buffer update ratio (0.1% in our setting), which likely mitigates the risk of overfitting in Q-function learning, thereby diminishing the benefit of dropout.

**Impact of Random Segment Lengths.** As showed in the previous ablation study, random segment length played a pivotal role in the strong performance of TOP-ERL. To further investigate whether this conclusion holds across different segment lengths, we evaluated the dense-reward Box Pushing task with segment lengths varying from 5% of the episode length to 100% (i.e., no segmentation). The results in Fig. 6 indicate that when using fixed-length segmentation, TOP-ERL’s performance varies significantly depending on the length. In contrast, random segment lengths consistently achieve faster convergence and higher asymptotic performance. Additionally, using random segmentation offers the practical benefit of simplifying hyperparameter tuning. Therefore, we adopt random segmentation length as the default setting for TOP-ERL. To provide more insight into the impact of random segment lengths, we provide a visualization for action correlation with different segmentation strategies in Appendix D.

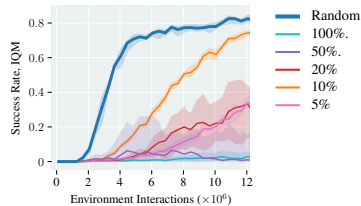


Figure 6: Random or Fixed segment length

## 6 CONCLUSION

This work introduced Transformer-based Off-Policy Episodic RL (TOP-ERL), a novel off-policy ERL method that leverages Transformers for N-steps return learning. By integrating ERL with an off-policy update scheme, TOP-ERL significantly improves the sample efficiency of ERL methods while retaining their advantages in exploration. The use of a Transformer-based critic architecture allows TOP-ERL to bypass the need for importance sampling in N-steps target calculation, stabilizing training while enjoying the benefit of low-bias value estimation provided by N-steps return. TOP-ERL has demonstrated superior performance compared to state-of-the-art ERL approaches and step-based RL methods augmented with exploration mechanism across 53 challenging tasks, providing strong evidence for its broader applicability to wide range of problems. The ablation studies reveal the reasons behind design choices and components, providing insights into the factors contributing to the strong performance of TOP-ERL.

**Limitations and Future Works.** Despite all the advantages, TOP-ERL shares a limitation common to ERL methods: it generates trajectories only at the start of each episode, making it incapable of handling tasks involving dynamic or target changes within an episode. A promising future research direction would be to incorporate replanning capabilities into TOP-ERL. Additionally, although TOP-ERL uses Transformers as critic, it is not designed to address POMDPs, as the Transformer is used for action-to-go processing in Q-function learning, rather than incorporating state sequences as input. Merging these two paradigms and enhancing TOP-ERL with the ability to handle POMDPs presents another avenue for future investigation.

540 7 ETHICS STATEMENT

541

542 No human participants were involved in this study. All data used in this work was generated through  
543 simulations. As such, there are no privacy or security concerns related to personal or sensitive  
544 information. We acknowledge the importance of fairness in AI and have taken care to ensure that  
545 our methodology does not introduce bias in simulated environments, though broader fairness issues  
546 in real-world applications of such models should be considered in future work. There are no conflicts  
547 of interest or sponsorship concerns associated with this research, and all practices adhere to legal  
548 and ethical standards.

549

550 8 REPRODUCIBILITY STATEMENT

551

552 The considerable efforts were made to ensure that our work is fully reproducible. All relevant code,  
553 including the implementation of the proposed algorithms, simulation environments, and trained  
554 models, will be made available in an GitHub repository provided in the main paper. Detailed de-  
555 scriptions of the experimental setup, including hyperparameter configurations can be found in the  
556 appendix.

557

558

559

560

561

562

563

564

565

566

567

568

569

570

571

572

573

574

575

576

577

578

579

580

581

582

583

584

585

586

587

588

589

590

591

592

593

## REFERENCES

- 594  
595  
596 Abbas Abdolmaleki, Rudolf Lioutikov, Jan R Peters, Nuno Lau, Luis Pualo Reis, and Gerhard  
597 Neumann. Model-based relative entropy stochastic search. *Advances in Neural Information Pro-*  
598 *cessing Systems*, 28, 2015.
- 599  
600 Abbas Abdolmaleki, Bob Price, Nuno Lau, Luis Paulo Reis, and Gerhard Neumann. Contextual  
601 covariance matrix adaptation evolutionary strategies. International Joint Conferences on Artificial  
602 Intelligence Organization (IJCAI), 2017.
- 603  
604 Rishabh Agarwal, Max Schwarzer, Pablo Samuel Castro, Aaron Courville, and Marc G Bellemare.  
605 Deep reinforcement learning at the edge of the statistical precipice. *Advances in Neural Informa-*  
*tion Processing Systems*, 2021.
- 606  
607 Jimmy Lei Ba. Layer normalization. *arXiv preprint arXiv:1607.06450*, 2016.
- 608  
609 Shikhar Bahl, Mustafa Mukadam, Abhinav Gupta, and Deepak Pathak. Neural dynamic policies  
610 for end-to-end sensorimotor learning. *Advances in Neural Information Processing Systems*, 33:  
5058–5069, 2020.
- 611  
612 Homanga Bharadhwaj, Jay Vakil, Mohit Sharma, Abhinav Gupta, Shubham Tulsiani, and Vikash  
613 Kumar. Roboagent: Generalization and efficiency in robot manipulation via semantic augmenta-  
614 tions and action chunking. In *2024 IEEE International Conference on Robotics and Automation*  
*(ICRA)*, pp. 4788–4795. IEEE, 2024.
- 615  
616 Alex Braylan, Mark Hollenbeck, Elliot Meyerson, and Risto Miikkulainen. Frame skip is a pow-  
617 erful parameter for learning to play atari. In *Workshops at the twenty-ninth AAAI conference on*  
618 *artificial intelligence*, 2015.
- 619  
620 Onur Celik, Dongzhuoran Zhou, Ge Li, Philipp Becker, and Gerhard Neumann. Specializing ver-  
621 satile skill libraries using local mixture of experts. In *Conference on Robot Learning*, pp. 1423–  
1433. PMLR, 2022.
- 622  
623 Onur Celik, Aleksandar Taranovic, and Gerhard Neumann. Acquiring diverse skills using curricu-  
624 lum reinforcement learning with mixture of experts. In *Forty-first International Conference on*  
625 *Machine Learning*, 2024. URL <https://openreview.net/forum?id=9ZkUFSw1UH>.
- 626  
627 Yevgen Chebotar, Quan Vuong, Karol Hausman, Fei Xia, Yao Lu, Alex Irpan, Aviral Kumar, Tianhe  
628 Yu, Alexander Herzog, Karl Pertsch, et al. Q-transformer: Scalable offline reinforcement learning  
629 via autoregressive q-functions. In *Conference on Robot Learning*, pp. 3909–3928. PMLR, 2023.
- 630  
631 Lili Chen, Kevin Lu, Aravind Rajeswaran, Kimin Lee, Aditya Grover, Misha Laskin, Pieter Abbeel,  
632 Aravind Srinivas, and Igor Mordatch. Decision transformer: Reinforcement learning via sequence  
modeling. *Advances in neural information processing systems*, 34:15084–15097, 2021.
- 633  
634 Onno Eberhard, Jakob Hollenstein, Cristina Pinneri, and Georg Martius. Pink noise is all you  
635 need: Colored noise exploration in deep reinforcement learning. In *The Eleventh International*  
*Conference on Learning Representations*, 2022.
- 636  
637 Scott Fujimoto, Herke Hoof, and David Meger. Addressing function approximation error in actor-  
638 critic methods. In *International conference on machine learning*, pp. 1587–1596. PMLR, 2018.
- 639  
640 Faustino Gomez, Jürgen Schmidhuber, Risto Miikkulainen, and Melanie Mitchell. Accelerated neu-  
641 ral evolution through cooperatively coevolved synapses. *Journal of Machine Learning Research*,  
9(5), 2008.
- 642  
643 Sebastian Gomez-Gonzalez, Gerhard Neumann, Bernhard Schölkopf, and Jan Peters. Using prob-  
644 abilistic movement primitives for striking movements. In *2016 IEEE-RAS 16th International*  
645 *Conference on Humanoid Robots (Humanoids)*, pp. 502–508. IEEE, 2016.
- 646  
647 Tuomas Haarnoja, Aurick Zhou, Pieter Abbeel, and Sergey Levine. Soft actor-critic: Off-policy  
maximum entropy deep reinforcement learning with a stochastic actor. In *International confer-*  
*ence on machine learning*, pp. 1861–1870. PMLR, 2018a.

- 648 Tuomas Haarnoja, Aurick Zhou, Kristian Hartikainen, George Tucker, Sehoon Ha, Jie Tan, Vikash  
649 Kumar, Henry Zhu, Abhishek Gupta, Pieter Abbeel, et al. Soft actor-critic algorithms and appli-  
650 cations. *arXiv preprint arXiv:1812.05905*, 2018b.
- 651 Shengyi Huang, Rousslan Fernand Julien Dossa, Antonin Raffin, Anssi Kanervisto, and Weixun  
652 Wang. The 37 implementation details of proximal policy optimization. *The ICLR Blog Track*  
653 *2023*, 2022.
- 654 Christian Igel. Neuroevolution for reinforcement learning using evolution strategies. In *The 2003*  
655 *Congress on Evolutionary Computation, 2003. CEC'03.*, volume 4, pp. 2588–2595. IEEE, 2003.
- 656 Auke Jan Ijspeert, Jun Nakanishi, Heiko Hoffmann, Peter Pastor, and Stefan Schaal. Dynamical  
657 movement primitives: learning attractor models for motor behaviors. *Neural computation*, 25(2):  
658 328–373, 2013.
- 659 Piotr Kicki, Davide Tateo, Puze Liu, Jonas Günster, Jan Peters, and Krzysztof Walas. Bridging  
660 the gap between learning-to-plan, motion primitives and safe reinforcement learning. In *8th An-  
661 nual Conference on Robot Learning*, 2024. URL [https://openreview.net/forum?id=](https://openreview.net/forum?id=ZdgaF8f0c0)  
662 [ZdgaF8f0c0](https://openreview.net/forum?id=ZdgaF8f0c0).
- 663 Jens Kober and Jan Peters. Policy search for motor primitives in robotics. *Advances in neural*  
664 *information processing systems*, 21, 2008.
- 665 Ge Li, Zeqi Jin, Michael Volpp, Fabian Otto, Rudolf Lioutikov, and Gerhard Neumann. ProdmP:  
666 A unified perspective on dynamic and probabilistic movement primitives. *IEEE Robotics and*  
667 *Automation Letters*, 8(4):2325–2332, 2023.
- 668 Ge Li, Hongyi Zhou, Dominik Roth, Serge Thilges, Fabian Otto, Rudolf Lioutikov, and Gerhard  
669 Neumann. Open the black box: Step-based policy updates for temporally-correlated episodic  
670 reinforcement learning. In *The Twelfth International Conference on Learning Representations*,  
671 2024. URL <https://openreview.net/forum?id=mnipav175N>.
- 672 Eric Liang, Richard Liaw, Robert Nishihara, Philipp Moritz, Roy Fox, Ken Goldberg, Joseph Gon-  
673 zalez, Michael Jordan, and Ion Stoica. Rllib: Abstractions for distributed reinforcement learning.  
674 In *International conference on machine learning*, pp. 3053–3062. PMLR, 2018.
- 675 Haoxin Lin, Yihao Sun, Jiayi Zhang, and Yang Yu. Model-based reinforcement learning with multi-  
676 step plan value estimation. In *ECAI 2023*, pp. 1481–1488. IOS Press, 2023.
- 677 Chenhao Lu, Ruizhe Shi, Yuyao Liu, Kaizhe Hu, Simon Shaolei Du, and Huazhe Xu. Rethinking  
678 transformers in solving POMDPs. In *Forty-first International Conference on Machine Learning*,  
679 2024. URL <https://openreview.net/forum?id=SyY7ScNpGL>.
- 680 Xiao Ma and Wu-Jun Li. Weighting online decision transformer with episodic memory for offline-  
681 to-online reinforcement learning. In *2024 IEEE International Conference on Robotics and Au-  
682 tomation (ICRA)*, pp. 10793–10799. IEEE, 2024.
- 683 Guilherme Maeda, Marco Ewerton, Rudolf Lioutikov, Heni Ben Amor, Jan Peters, and Gerhard  
684 Neumann. Learning interaction for collaborative tasks with probabilistic movement primitives.  
685 In *2014 IEEE-RAS International Conference on Humanoid Robots*, pp. 527–534. IEEE, 2014.
- 686 Horia Mania, Aurelia Guy, and Benjamin Recht. Simple random search of static linear policies is  
687 competitive for reinforcement learning. *Advances in Neural Information Processing Systems*, 31,  
688 2018.
- 689 Volodymyr Mnih, Koray Kavukcuoglu, David Silver, Andrei A Rusu, Joel Veness, Marc G Belle-  
690 mare, Alex Graves, Martin Riedmiller, Andreas K Fidjeland, Georg Ostrovski, et al. Human-level  
691 control through deep reinforcement learning. *nature*, 518(7540):529–533, 2015.
- 692 Tianwei Ni, Michel Ma, Benjamin Eysenbach, and Pierre-Luc Bacon. When do transformers shine  
693 in rl? decoupling memory from credit assignment. *Advances in Neural Information Processing*  
694 *Systems*, 36, 2024.

- 702 Toshihiro Ota. Decision mamba: Reinforcement learning via sequence modeling with selective state  
703 spaces. *arXiv preprint arXiv:2403.19925*, 2024.
- 704 Fabian Otto, Onur Celik, Dominik Roth, and Hongyi Zhou. Fancy gym. URL [https://github.com/ALRhub/fancy\\_gym](https://github.com/ALRhub/fancy_gym).
- 705 Fabian Otto, Philipp Becker, Ngo Anh Vien, Hanna Carolin Ziesche, and Gerhard Neumann. Differ-  
706 entiable trust region layers for deep reinforcement learning. *International Conference on Learning  
707 Representations*, 2021.
- 708 Fabian Otto, Onur Celik, Hongyi Zhou, Hanna Ziesche, Vien Anh Ngo, and Gerhard Neumann. Deep  
709 black-box reinforcement learning with movement primitives. In *Conference on Robot  
710 Learning*, pp. 1244–1265. PMLR, 2022.
- 711 Fabian Otto, Hongyi Zhou, Onur Celik, Ge Li, Rudolf Lioutikov, and Gerhard Neumann. Mp3:  
712 Movement primitive-based (re-) planning policy. *arXiv preprint arXiv:2306.12729*, 2023.
- 713 Rok Pahič, Barry Ridge, Andrej Gams, Jun Morimoto, and Aleš Ude. Training of deep neural  
714 networks for the generation of dynamic movement primitives. *Neural Networks*, 2020.
- 715 Alexandros Paraschos, Christian Daniel, Jan Peters, and Gerhard Neumann. Probabilistic movement  
716 primitives. *Advances in neural information processing systems*, 26, 2013.
- 717 Emilio Parisotto, Francis Song, Jack Rae, Razvan Pascanu, Caglar Gulcehre, Siddhant Jayakumar,  
718 Max Jaderberg, Raphael Lopez Kaufman, Aidan Clark, Seb Noury, et al. Stabilizing transformers  
719 for reinforcement learning. In *International conference on machine learning*, pp. 7487–7498.  
720 PMLR, 2020.
- 721 Jan Peters and Stefan Schaal. Reinforcement learning of motor skills with policy gradients. *Neural  
722 networks*, 21(4):682–697, 2008.
- 723 Kai Ploeger, Michael Lutter, and Jan Peters. High acceleration reinforcement learning for real-world  
724 juggling with binary rewards. In *Conference on Robot Learning*, pp. 642–653. PMLR, 2021.
- 725 Antonin Raffin, Ashley Hill, Adam Gleave, Anssi Kanervisto, Maximilian Ernestus, and Noah  
726 Dormann. Stable-baselines3: Reliable reinforcement learning implementations. *Journal of  
727 Machine Learning Research*, 22(268):1–8, 2021. URL [http://jmlr.org/papers/v22/  
728 20-1364.html](http://jmlr.org/papers/v22/20-1364.html).
- 729 Antonin Raffin, Jens Kober, and Freek Stulp. Smooth exploration for robotic reinforcement learning.  
730 In *Conference on Robot Learning*, pp. 1634–1644. PMLR, 2022.
- 731 Moritz Reuss, Ömer Erdinç Yağmurlu, Fabian Wenzel, and Rudolf Lioutikov. Multimodal diffu-  
732 sion transformer: Learning versatile behavior from multimodal goals. In *Robotics: Science and  
733 Systems*, 2024.
- 734 Leonel Rozo and Vedant Dave. Orientation probabilistic movement primitives on riemannian man-  
735 ifolds. In *Conference on Robot Learning*, pp. 373–383. PMLR, 2022.
- 736 Thomas Rückstieß, Martin Felder, and Jürgen Schmidhuber. State-dependent exploration for pol-  
737 icy gradient methods. In Walter Daelemans, Bart Goethals, and Katharina Morik (eds.), *Ma-  
738 chine Learning and Knowledge Discovery in Databases*, pp. 234–249, Berlin, Heidelberg, 2008.  
739 Springer Berlin Heidelberg. ISBN 978-3-540-87481-2.
- 740 Thomas Rückstieß, Frank Sehnke, Tom Schaul, Daan Wierstra, Yi Sun, and Jürgen Schmidhuber.  
741 Exploring parameter space in reinforcement learning. *Paladyn*, 1:14–24, 2010.
- 742 Tim Salimans, Jonathan Ho, Xi Chen, Szymon Sidor, and Ilya Sutskever. Evolution strategies as a  
743 scalable alternative to reinforcement learning. *arXiv preprint arXiv:1703.03864*, 2017.
- 744 Stefan Schaal. Dynamic movement primitives—a framework for motor control in humans and hu-  
745 manoid robotics. In *Adaptive motion of animals and machines*, pp. 261–280. Springer, 2006.
- 746 John Schulman, Filip Wolski, Prafulla Dhariwal, Alec Radford, and Oleg Klimov. Proximal policy  
747 optimization algorithms. *arXiv preprint arXiv:1707.06347*, 2017.

- 756 RB Ashith Shyam, Peter Lightbody, Gautham Das, Pengcheng Liu, Sebastian Gomez-Gonzalez,  
757 and Gerhard Neumann. Improving local trajectory optimisation using probabilistic movement  
758 primitives. In *2019 IEEE/RSJ International Conference on Intelligent Robots and Systems (IROS)*,  
759 pp. 2666–2671. IEEE, 2019.
- 760 Richard S Sutton. Learning to predict by the methods of temporal differences. *Machine learning*,  
761 3:9–44, 1988.
- 762 Richard S Sutton and Andrew G Barto. *Reinforcement learning: An introduction*. MIT press, 2018.
- 763 Jens Timmer and Michel Koenig. On generating power law noise. *Astronomy and Astrophysics*,  
764 300:707, 1995.
- 765 A Vaswani. Attention is all you need. *Advances in Neural Information Processing Systems*, 2017.
- 766 Darrell Whitley, Stephen Dominic, Rajarshi Das, and Charles W Anderson. Genetic reinforcement  
767 learning for neurocontrol problems. *Machine Learning*, 13:259–284, 1993.
- 768 Yueh-Hua Wu, Xiaolong Wang, and Masashi Hamaya. Elastic decision transformer. *Advances in  
769 Neural Information Processing Systems*, 36, 2024.
- 770 Taku Yamagata, Ahmed Khalil, and Raul Santos-Rodriguez. Q-learning decision transformer:  
771 Leveraging dynamic programming for conditional sequence modelling in offline rl. In *Inter-  
772 national Conference on Machine Learning*, pp. 38989–39007. PMLR, 2023.
- 773 Tianhe Yu, Deirdre Quillen, Zhanpeng He, Ryan Julian, Karol Hausman, Chelsea Finn, and Sergey  
774 Levine. Meta-world: A benchmark and evaluation for multi-task and meta reinforcement learning.  
775 In *Conference on robot learning*, pp. 1094–1100. PMLR, 2020.
- 776 Weilin Yuan, Jiaying Chen, Shaofei Chen, Dawei Feng, Zhenzhen Hu, Peng Li, and Weiwei Zhao.  
777 Transformer in reinforcement learning for decision-making: a survey. *Frontiers of Information  
778 Technology & Electronic Engineering*, 25(6):763–790, 2024.
- 779 Haichao Zhang, We Xu, and Haonan Yu. Policy expansion for bridging offline-to-online reinforce-  
780 ment learning. *arXiv preprint arXiv:2302.00935*, 2023.
- 781 Tony Z Zhao, Vikash Kumar, Sergey Levine, and Chelsea Finn. Learning fine-grained bimanual  
782 manipulation with low-cost hardware. *arXiv preprint arXiv:2304.13705*, 2023.
- 783 Qinqing Zheng, Amy Zhang, and Aditya Grover. Online decision transformer. In *international  
784 conference on machine learning*, pp. 27042–27059. PMLR, 2022.
- 785 You Zhou, Jianfeng Gao, and Tamim Asfour. Learning via-point movement primitives with inter-  
786 and extrapolation capabilities. In *2019 IEEE/RSJ International Conference on Intelligent Robots  
787 and Systems (IROS)*, pp. 4301–4308. IEEE, 2019.
- 788  
789  
790  
791  
792  
793  
794  
795  
796  
797  
798  
799  
800  
801  
802  
803  
804  
805  
806  
807  
808  
809

## List of Content in Appendix

- A. Options for the future return in Table 2.
- B. Mathematical formulations of MP methods used for trajectory generation.
- C. Experiment settings as a complementary to Sec. 5.
- D. Action Correlation Visualization.
- E. Hyper-parameters selection and sweeping.

### A TARGET OPTIONS

Table 2: Options for the future return used in Eq.(8)

| Option          | Math                                     | Description                     |
|-----------------|--|---------------------------------|
| <b>V-target</b> | $V_{\phi}^{\text{tar}}(s_N)$             | State value after N steps       |
| <b>Q-target</b> | $Q_{\phi}^{\text{tar}}(s_N, a_N, \dots)$ | Action value after N steps      |
| <b>Clipped</b>  | $\text{Min}(\cdot, \cdot)$               | Minimum of 2 target critics     |
| <b>Ensemble</b> | $\text{Avg}(\cdot, \cdot)$               | Mean of $\geq 2$ target critics |

### B MATHEMATICAL FORMULATIONS OF MOVEMENT PRIMITIVES.

In this section, we provide an overview of the movement primitive formulations used in this paper. We begin with the basics of DMPs and ProMPs, followed by a detailed explanation of ProDMPs. For clarity, we start with a single DoF system and then expand to multi-DoF systems.

#### B.1 DYNAMIC MOVEMENT PRIMITIVES (DMPs)

Schaal (2006); Ijspeert et al. (2013) describe a single movement as a trajectory  $[y_t]_{t=0:T}$ , which is governed by a second-order linear dynamical system with a non-linear forcing function  $f$ . The mathematical representation is given by

$$\tau^2 \ddot{y} = \alpha(\beta(g - y) - \tau \dot{y}) + f(x), \quad f(x) = x \frac{\sum \varphi_i(x) w_i}{\sum \varphi_i(x)} = x \boldsymbol{\varphi}_x^T \mathbf{w}, \quad (10)$$

where  $y = y(t)$ ,  $\dot{y} = dy/dt$ ,  $\ddot{y} = d^2y/dt^2$  denote the position, velocity, and acceleration of the system at a specific time  $t$ , respectively. Constants  $\alpha$  and  $\beta$  are spring-damper parameters,  $g$  signifies a goal attractor, and  $\tau$  is a time constant that modulates the speed of trajectory execution. To ensure convergence towards the goal, DMPs employ a forcing function governed by an exponentially decaying phase variable  $x(t) = \exp(-\alpha_x/\tau; t)$ . Here,  $\varphi_i(x)$  represents the basis functions for the forcing term. The trajectory’s shape as it approaches the goal is determined by the weight parameters  $w_i \in \mathbf{w}$ , for  $i = 1, \dots, N$ . The trajectory  $[y_t]_{t=0:T}$  is typically computed by numerically integrating the dynamical system from the start to the end point (Pahič et al., 2020; Bahl et al., 2020). However, this numerical process is computationally intensive. For example, to compute the trajectory segment in the end of an episode, DMP must integrate the system from the very beginning till the start of the segment.

#### B.2 PROBABILISTIC MOVEMENT PRIMITIVES (PROMPs)

Paraschos et al. (2013) introduced a framework for modeling MPs using trajectory distributions, capturing both temporal and inter-dimensional correlations. Unlike DMPs that use a forcing term, ProMPs directly model the intended trajectory. The probability of observing a 1-DoF trajectory

$[y_t]_{t=0:T}$  given a specific weight vector distribution  $p(\mathbf{w}) \sim \mathcal{N}(\mathbf{w}|\boldsymbol{\mu}_w, \boldsymbol{\Sigma}_w)$  is represented as a linear basis function model:

$$\text{Linear basis function: } [y_t]_{t=0:T} = \boldsymbol{\Phi}_{0:T}^\top \mathbf{w} + \epsilon_y, \quad (11)$$

$$\text{Mapping distribution: } p([y_t]_{t=0:T}; \boldsymbol{\mu}_y, \boldsymbol{\Sigma}_y) = \mathcal{N}(\boldsymbol{\Phi}_{0:T}^\top \boldsymbol{\mu}_w, \boldsymbol{\Phi}_{0:T}^\top \boldsymbol{\Sigma}_w \boldsymbol{\Phi}_{0:T} + \sigma_y^2 \mathbf{I}). \quad (12)$$

Here,  $\epsilon_y$  is zero-mean white noise with variance  $\sigma_y^2$ . The matrix  $\boldsymbol{\Phi}_{0:T}$  houses the basis functions for each time step  $t$ . Similar to DMPs, these basis functions can be defined in terms of a phase variable instead of time. ProMPs allows for flexible manipulation of MP trajectories through probabilistic operators applied to  $p(\mathbf{w})$ , such as conditioning, combination, and blending (Maeda et al., 2014; Gomez-Gonzalez et al., 2016; Shyam et al., 2019; Rozo & Dave, 2022; Zhou et al., 2019). However, ProMPs lack an intrinsic dynamic system, which means they cannot guarantee a smooth transition from the robot’s initial state or between different generated trajectories.

### B.3 PROBABILISTIC DYNAMIC MOVEMENT PRIMITIVES (PRODMPs)

**Solving the ODE underlying DMPs** Li et al. (2023) noted that the governing equation of DMPs, as specified in Eq. (10), admits an analytical solution. This is because it is a second-order linear non-homogeneous ODE with constant coefficients. The original ODE and its homogeneous counterpart can be expressed in standard form as follows:

$$\text{Non-homo. ODE: } \ddot{y} + \frac{\alpha}{\tau} \dot{y} + \frac{\alpha\beta}{\tau^2} y = \frac{f(x)}{\tau^2} + \frac{\alpha\beta}{\tau^2} g \equiv F(x, g), \quad (13)$$

$$\text{Homo. ODE: } \ddot{y} + \frac{\alpha}{\tau} \dot{y} + \frac{\alpha\beta}{\tau^2} y = 0. \quad (14)$$

The solution to this ODE is essentially the position trajectory, and its time derivative yields the velocity trajectory. These are formulated as:

$$y = [y_2 \mathbf{p}_2 - y_1 \mathbf{p}_1 \quad y_2 q_2 - y_1 q_1] \begin{bmatrix} \mathbf{w} \\ g \end{bmatrix} + c_1 y_1 + c_2 y_2 \quad (15)$$

$$\dot{y} = [\dot{y}_2 \mathbf{p}_2 - \dot{y}_1 \mathbf{p}_1 \quad \dot{y}_2 q_2 - \dot{y}_1 q_1] \begin{bmatrix} \mathbf{w} \\ g \end{bmatrix} + c_1 \dot{y}_1 + c_2 \dot{y}_2. \quad (16)$$

Here, the learnable parameters  $\mathbf{w}$  and  $g$  which control the shape of the trajectory, are separable from the remaining terms. Time-dependent functions  $y_1, y_2, \mathbf{p}_1, \mathbf{p}_2, q_1, q_2$  in the remaining terms offer the basic support to generate the trajectory. The functions  $y_1, y_2$  are the complementary solutions to the homogeneous ODE presented in equation 14, and  $\dot{y}_1, \dot{y}_2$  their time derivatives respectively. These time-dependent functions take the form as:

$$y_1(t) = \exp\left(-\frac{\alpha}{2\tau}t\right), \quad y_2(t) = t \exp\left(-\frac{\alpha}{2\tau}t\right), \quad (17)$$

$$\mathbf{p}_1(t) = \frac{1}{\tau^2} \int_0^t t' \exp\left(\frac{\alpha}{2\tau}t'\right) x(t') \boldsymbol{\varphi}_x^\top dt', \quad \mathbf{p}_2(t) = \frac{1}{\tau^2} \int_0^t \exp\left(\frac{\alpha}{2\tau}t'\right) x(t') \boldsymbol{\varphi}_x^\top dt', \quad (18)$$

$$q_1(t) = \left(\frac{\alpha}{2\tau}t - 1\right) \exp\left(\frac{\alpha}{2\tau}t\right) + 1, \quad q_2(t) = \frac{\alpha}{2\tau} \left[ \exp\left(\frac{\alpha}{2\tau}t\right) - 1 \right]. \quad (19)$$

It’s worth noting that the  $\mathbf{p}_1$  and  $\mathbf{p}_2$  cannot be analytically derived due to the complex nature of the forcing basis terms  $\boldsymbol{\varphi}_x$ . As a result, they need to be computed numerically. Despite this, isolating the learnable parameters, namely  $\mathbf{w}$  and  $g$ , allows for the reuse of the remaining terms across all generated trajectories. These residual terms can be more specifically identified as the position and velocity basis functions, denoted as  $\boldsymbol{\Phi}(t)$  and  $\dot{\boldsymbol{\Phi}}(t)$ , respectively. When both  $\mathbf{w}$  and  $g$  are included in a concatenated vector, represented as  $\mathbf{w}_g$ , the expressions for position and velocity trajectories can be formulated in a manner akin to that employed by ProMPs:

$$\text{Position: } y(t) = \boldsymbol{\Phi}(t)^\top \mathbf{w}_g + c_1 y_1(t) + c_2 y_2(t), \quad (20)$$

$$\text{Velocity: } \dot{y}(t) = \dot{\boldsymbol{\Phi}}(t)^\top \mathbf{w}_g + c_1 \dot{y}_1(t) + c_2 \dot{y}_2(t). \quad (21)$$

In the main paper, for simplicity and notation convenience, we use  $\mathbf{w}$  instead of  $\mathbf{w}_g$  to describe the parameters and goal of ProDMPs.

**Initial Condition Enforcement** The coefficients  $c_1$  and  $c_2$  serve as solutions to the initial value problem delineated by the Eq.(20)(21). Li et al. propose utilizing the robot’s initial state or the replanning state, characterized by the robot’s position and velocity  $(y_b, \dot{y}_b)$  to ensure a smooth commencement or transition from a previously generated trajectory. Denote the values of the complementary functions and their derivatives at the condition time  $t_b$  as  $y_{1_b}, y_{2_b}, \dot{y}_{1_b}$  and  $\dot{y}_{2_b}$ . Similarly, denote the values of the position and velocity basis functions at this time as  $\Phi_b$  and  $\dot{\Phi}_b$  respectively. Using these notations,  $c_1$  and  $c_2$  can be calculated as follows:

$$\begin{bmatrix} c_1 \\ c_2 \end{bmatrix} = \begin{bmatrix} \frac{\dot{y}_{2_b} y_b - y_{2_b} \dot{y}_b}{y_{1_b} \dot{y}_{2_b} - y_{2_b} \dot{y}_{1_b}} + \frac{y_{2_b} \dot{\Phi}_b^\top - \dot{y}_{2_b} \Phi_b^\top}{y_{1_b} \dot{y}_{2_b} - y_{2_b} \dot{y}_{1_b}} \mathbf{w}_g \\ \frac{y_{1_b} \dot{y}_b - \dot{y}_{1_b} y_b}{y_{1_b} \dot{y}_{2_b} - y_{2_b} \dot{y}_{1_b}} + \frac{\dot{y}_{1_b} \Phi_b^\top - y_{1_b} \dot{\Phi}_b^\top}{y_{1_b} \dot{y}_{2_b} - y_{2_b} \dot{y}_{1_b}} \mathbf{w}_g \end{bmatrix}. \quad (22)$$

Substituting Eq. (22) into Eq. (20) and Eq. (21), the position and velocity trajectories take the form as

$$y = \xi_1 y_b + \xi_2 \dot{y}_b + [\xi_3 \Phi_b + \xi_4 \dot{\Phi}_b + \Phi]^\top \mathbf{w}_g, \quad (23)$$

$$\dot{y} = \dot{\xi}_1 y_b + \dot{\xi}_2 \dot{y}_b + [\dot{\xi}_3 \Phi_b + \dot{\xi}_4 \dot{\Phi}_b + \dot{\Phi}]^\top \mathbf{w}_g \quad (24)$$

Here,  $\xi_k$  for  $k \in \{1, 2, 3, 4\}$  serve as intermediate terms that are derived from the complementary functions and the initial conditions. The formations of these terms are elaborated below. To find their derivatives  $\dot{\xi}_k$ , one can simply replace  $y_1, y_2$  with their time derivatives  $\dot{y}_1, \dot{y}_2$  in the equations.

$$\begin{aligned} \xi_1(t) &= \frac{\dot{y}_{2_b} y_1 - \dot{y}_{1_b} y_2}{y_{1_b} \dot{y}_{2_b} - y_{2_b} \dot{y}_{1_b}}, & \xi_2(t) &= \frac{y_{1_b} y_2 - y_{2_b} y_1}{y_{1_b} \dot{y}_{2_b} - y_{2_b} \dot{y}_{1_b}}, \\ \xi_3(t) &= \frac{\dot{y}_{1_b} y_2 - \dot{y}_{2_b} y_1}{y_{1_b} \dot{y}_{2_b} - y_{2_b} \dot{y}_{1_b}}, & \xi_4(t) &= \frac{y_{2_b} y_1 - y_{1_b} y_2}{y_{1_b} \dot{y}_{2_b} - y_{2_b} \dot{y}_{1_b}}. \end{aligned}$$

Despite the complex form used in the initial condition enforcement, the solutions conducted above only rely on solving several linear equations and can be easily implemented in a batch-manner and is therefore computationally efficient, normally  $\leq 1$  ms.

## C EXPERIMENT DETAILS

### C.1 DETAILS OF METHODS IMPLEMENTATION

Table 3: Baseline methods categorized by type (ERL or SRL) and update rules (On- or Off-policy).

| Method                                | Category | Description  |
|---------------------------------------|----------|--|
| <b>BBRL</b> (Otto et al., 2022)       | ERL, On  | Black Box Optimization style ERL, policy search in parameter space   |
| <b>TCE</b> (Li et al., 2024)          | ERL, On  | Extend BBRL to use per-step info for efficient policy update         |
| <b>PPO</b> (Schulman et al., 2017)    | SRL, On  | Standard on-policy method with simplified Trust Region enforcement   |
| <b>gSDE</b> (Raffin et al., 2022)     | SRL, On  | Consecutive exploration noise for NN parameters of the policy        |
| <b>GTrXL</b> (Parisotto et al., 2020) | SRL, On  | <u>Transformer</u> -augmented SRL with multiple state as history     |
| <b>SAC</b> (Haarnoja et al., 2018a)   | SRL, Off | Standard off-policy method with entropy bonus for better exploration |
| <b>PINK</b> (Eberhard et al., 2022)   | SRL, Off | Use temporal correlated pink noise for better exploration            |

**PPO** Proximal Policy Optimization (PPO) (Schulman et al., 2017) is a prominent on-policy step-based RL algorithm that refines the policy gradient objective, ensuring policy updates remain close to the behavior policy. PPO branches into two main variants: PPO-Penalty, which incorporates a KL-divergence term into the objective for regularization, and PPO-Clip, which employs a clipped surrogate objective. In this study, we focus our comparisons on PPO-Clip due to its prevalent use in the field. Our implementation of PPO is based on the implementation of Raffin et al. (2021).

**SAC** Soft Actor-Critic (SAC) (Haarnoja et al., 2018a;b) employs a stochastic step-based policy in an off-policy setting and utilizes double Q-networks to mitigate the overestimation of Q-values for stable updates. By integrating entropy regularization into the learning objective, SAC balances between expected returns and policy entropy, preventing the policy from premature convergence. Our implementation of SAC is based on the implementation of Raffin et al. (2021).

**GTrXL** Gated TransformerXL (GTrXL) (Parisotto et al., 2020) is a Transformer architecture that design to stabilize the training of Transformers in online RL, offers an easy-to-train, simple-to-implement but substantially more expressive architectural alternative to standard RNNs used for RL agents in POMDPs. Our implementation of GTrXL is based on the implementation of PPO + GTrXL from Liang et al. (2018). We augmented the implementation with minibatch advantage normalization and state-independent log standard deviation as suggested in Huang et al. (2022).

**gSDE** Generalized State Dependent Exploration (gSDE) (Raffin et al., 2022; Rückstieß et al., 2008; Rückstieß et al., 2010) is an exploration method designed to address issues with traditional step-based exploration techniques and aims to provide smoother and more efficient exploration in the context of robotic reinforcement learning, reducing jerky motion patterns and potential damage to robot motors while maintaining competitive performance in learning tasks.

To achieve this, gSDE replaces the traditional approach of independently sampling from a Gaussian noise at each time step with a more structured exploration strategy, that samples in a state-dependent manner. The generated samples not only depend on parameter of the Gaussian distribution  $\mu$  &  $\Sigma$ , but also on the activations of the policy network’s last hidden layer ( $s$ ). We generate disturbances  $\epsilon_t$  using the equation

$$\epsilon_t = \theta_\epsilon s, \text{ where } \theta_\epsilon \sim \mathcal{N}^d(0, \Sigma).$$

The exploration matrix  $\theta_\epsilon$  is composed of vectors of length  $\text{Dim}(a)$  that were drawn from the Gaussian distribution we want gSDE to follow. The vector  $s$  describes how this set of pre-computed exploration vectors are mixed. The exploration matrix is resampled at regular intervals, as guided by the ‘sde sampling frequency’ (ssf), occurring every n-th step if n is our ssf.

gSDE is versatile, applicable as a substitute for the Gaussian Noise source in numerous on- and off-policy algorithms. We evaluated its performance in an on-policy setting using PPO by utilizing the reference implementation for gSDE from Raffin et al. (2022). In order for training with gSDE to

1026 remain stable and reach high performance the usage of a linear schedule over the clip range had to  
 1027 be used for some environments.

1028  
 1029 **PINK** We utilize SAC to evaluate the effectiveness of pink noise for efficient exploration. Eber-  
 1030 hard et al. (2022) propose to replace the independent action noise  $\epsilon_t$  of

$$1031 \quad a_t = \mu_t + \sigma_t \cdot \epsilon_t$$

1032  
 1033 with correlated noise from particular random processes, whose power spectral density fol-  
 1034 low a power law. In particular, the use of pink noise, with the exponent  $\beta = 1$  in  
 1035  $S(f) = |\mathcal{F}[\epsilon](f)|^2 \propto f^{-\beta}$ , should be considered (Eberhard et al., 2022).

1036  
 1037 We follow the reference implementation and sample chunks of Gaussian pink noise using the in-  
 1038 verse Fast Fourier Transform method proposed by Timmer & Koenig (1995). These noise variables  
 1039 are used for SAC’s exploration but the the actor and critic updates sample the independent action  
 1040 distribution without pink noise. Each action dimension uses an independent noise process which  
 1041 causes temporal correlation within each dimension but not across dimensions. Furthermore, we fix  
 1042 the chunk size and maximum period to 10000 which avoids frequent jumps of chunk borders and  
 1043 increases relative power of low frequencies.

1044 **BBRL** Black-Box Reinforcement Learning (BBRL) (Otto et al., 2022; 2023) is a recent developed  
 1045 episodic reinforcement learning method. By utilizing ProMPs (Paraschos et al., 2013) as the trajec-  
 1046 tory generator, BBRL learns a policy that explores at the trajectory level. The method can effectively  
 1047 handle sparse and non-Markovian rewards by perceiving an entire trajectory as a unified data point,  
 1048 neglecting the temporal structure within sampled trajectories. However, on the other hand, BBRL  
 1049 suffers from relatively low sample efficiency due to its black-box nature. Moreover, the original  
 1050 BBRL employs a degenerate Gaussian policy with diagonal covariance. In this study, we extend  
 1051 BBRL to learn Gaussian policy with full covariance to build a more competitive baseline. For clar-  
 1052 ity, we refer to the original method as BBRL-Std and the full covariance version as BBRL-Cov. We  
 1053 integrate BBRL with ProDMPs (Li et al., 2023), aiming to isolate the effects attributable to different  
 1054 MP approaches.

1055 **TCE** Temporally-Correlated Episodic RL (TCE) (Li et al., 2024) is an innovative ERL algorithm  
 1056 that leverages step-level information in episodic policy updates, shedding light on the ‘black box’  
 1057 of current ERL methods while preserving smooth and consistent exploration within the parameter  
 1058 space. TCE integrates the strengths of both step-based and episodic RL, offering performance on  
 1059 par with recent ERL approaches, while matching the data efficiency of state-of-the-art (SoTA) step-  
 1060 based RL methods.

## 1061 C.2 META WORLD

1062  
 1063 MetaWorld (Yu et al., 2020) is an open-source simulated benchmark specifically designed for meta-  
 1064 reinforcement learning and multi-task learning in robotic manipulation. It features 50 distinct ma-  
 1065 nipulation tasks, each presenting unique challenges that require robots to learn a wide range of skills,  
 1066 such as grasping, pushing, and object placement. Unlike benchmarks that focus on narrow task dis-  
 1067 tributions, MetaWorld provides a broader range of tasks, making it an ideal platform for developing  
 1068 algorithms that can generalize across different behaviors.

## 1069 C.3 HOPPER JUMP

1070  
 1071 As an addition to the main paper, we provide more details on the Hopper  
 1072 Jump task. We look at both the main goal of maximizing jump height and  
 1073 the secondary goal of landing on a desired position. Our method shows  
 1074 quick learning and does well in achieving high jump height, consistent  
 1075 with what we reported earlier. While it’s not as strong in landing accu-  
 1076 racy, it still ranks high in overall performance. Both versions of BBRL  
 1077 have similar results. However, they train more slowly compared to TCE,  
 1078 highlighting the speed advantage of our method due to the use of inter-  
 1079 mediate states for policy updates. Looking at other methods, step-based

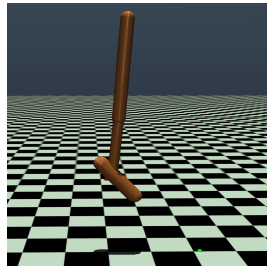


Figure 7: Hopper Jump

ones like PPO and TRPL focus too much on landing distance and miss out on jump height, leading to less effective policies. On the other hand, gSDE performs well but is sensitive to the initial setup, as shown by the wide confidence ranges in the results. Lastly, SAC and PINK shows inconsistent results in jump height, indicating the limitations of using pink noise for exploration, especially when compared to gSDE.

### C.4 BOX PUSHING

The goal of the box-pushing task is to move a box to a specified goal location and orientation using the 7-DoFs Franka Emika Panda (Otto et al., 2022). To make the environment more challenging, we extend the environment from a fixed initial box position and orientation to a randomized initial position and orientation. The range of both initial and target box pose varies from  $x \in [0.3, 0.6]$ ,  $y \in [-0.45, 0.45]$ ,  $\theta_z \in [0, 2\pi]$ . Success is defined as a positional distance error of less than 5 cm and a z-axis orientation error of less than 0.5 rad. We refer to the original paper for the observation and action spaces definition and the reward function.

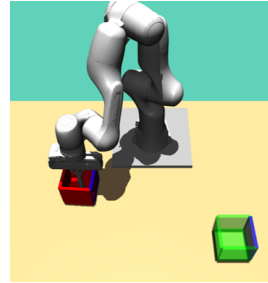


Figure 8: Box Pushing

### D ACTION CORRELATION WITH SEGMENTATION

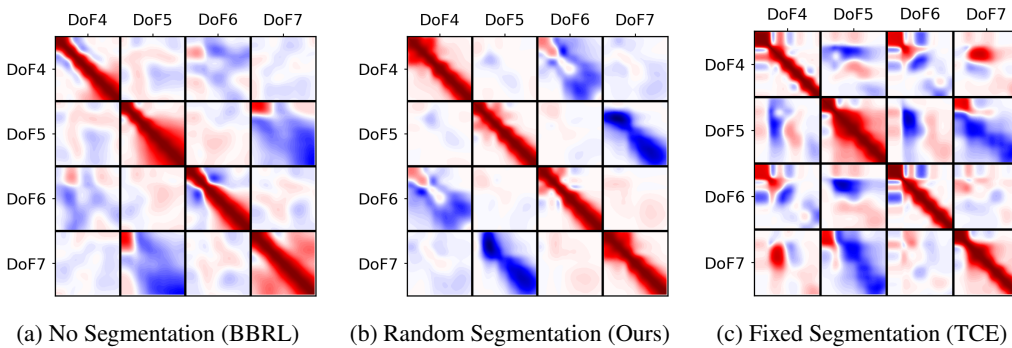


Figure 9: This figure presents predicted actions’ correlation across 4 DoF and 100 time steps, visualized in a  $400 \times 400$  correlation matrix. Each  $100 \times 100$  square tile demonstrates the movement correlation between two DoF during these steps. Correlation values range from -1 (negative correlation, depicted in blue) to 1 (positive correlation, depicted in red), with white areas indicating no correlation. BBRL treats the entire trajectory as a whole and does not have any segmentation; thus, the correlation broadcasts smoothly across time steps, as shown in (a). On the contrary, TCE uses segmentation with fixed length, constraining the correlation learning within fixed segments, resulting in sudden correlation changes at each segment’s boundary, as presented in (c). TOP-ERL utilizes randomly sampled segment length and positions itself between the two paradigms, being able to learn the smooth correlation while retaining the benefits of higher sample efficiency by using segmentation.

1134 E HYPER PARAMETERS  
1135

1136 We executed a large-scale grid search to fine-tune key hyperparameters for each baseline method.  
1137 For other hyperparameters, we relied on the values specified in their respective original papers.  
1138 Below is a list summarizing the parameters we swept through during this process.  
1139

1140 **BBRL:** Policy net size, critic net size, policy learning rate, critic learning rate, samples per itera-  
1141 tion, trust region dissimilarity bounds, number of parameters per movement DoF.  
1142

1143 **TCE:** Same types of hyper-parameters listed in BBRL, plus the number of segments per trajectory.  
1144 A learning rate decaying scheduler is applied to stabilize the training in the end.  
1145

1146 **PPO:** Policy network size, critic network size, policy learning rate, critic learning rate, batch size,  
1147 samples per iteration.  
1148

1149 **gSDE:** Same types of hyper-parameters listed in PPO, together with the state dependent explo-  
1150 ration sampling frequency (Raffin et al., 2022).  
1151

1152 **SAC:** Policy network size, critic network size, policy learning rate, critic learning rate, alpha learn-  
1153 ing rate, batch size, Update-To-Data (UTD) ratio.  
1154

1155 **PINK:** Same types of hyper-parameters listed in SAC.  
1156

1157 **GTrXL:** Number of multi-head attention layers, number of heads, dims per head, importance-  
1158 sampling ratio clip, value function clip, grad clip, and same hyperparameters listed in PPO  
1159

1160 **TOP-ERL:** Number of multi-head attention layers, number of heads, dims per head, learning  
1161 rates. The other movement primitives hyper-parameters are taken from TCE.

1162 The detailed hyper parameters used are listed in the following tables. Unless stated otherwise, the  
1163 notation  $\text{lin}_x$  refers to a linear schedule. It interpolates linearly from  $x$  to 0 during training. The  
1164 ERL methods (TCE, BBRL) take an entire trajectory as a sample where the SRL methods take one  
1165 time step as a sample. In this way, one sample in ERL is equivalent to  $T$  sample of SRL, where  $T$  is  
1166 the length of one task episode.  
1167  
1168  
1169  
1170  
1171  
1172  
1173  
1174  
1175  
1176  
1177  
1178  
1179  
1180  
1181  
1182  
1183  
1184  
1185  
1186  
1187

Table 4: Hyperparameters for the Meta-World experiments. Episode Length  $T = 500$ 

|                            | PPO        | gSDE       | GTrXL  | SAC        | PINK       | TCE        | BBRL     | TOP-ERL    |
|----------------------------|------------|------------|--------|------------|------------|------------|----------|------------|
| number samples             | 16000      | 16000      | 19000  | 1000       | 4          | 16         | 16       | 2          |
| GAE $\lambda$              | 0.95       | 0.95       | 0.95   | n.a.       | n.a.       | 0.95       | n.a.     | n.a.       |
| discount factor            | 0.99       | 0.99       | 0.99   | 0.99       | 0.99       | 1          | 1        | 1.0        |
| $\epsilon_\mu$             | n.a.       | n.a.       | n.a.   | n.a.       | n.a.       | 0.005      | 0.005    | 0.005      |
| $\epsilon_\Sigma$          | n.a.       | n.a.       | n.a.   | n.a.       | n.a.       | 0.0005     | 0.0005   | 0.0005     |
| trust region loss coef.    | n.a.       | n.a.       | n.a.   | n.a.       | n.a.       | 1          | 10       | 1.0        |
| optimizer                  | adam       | adam       | adam   | adam       | adam       | adam       | adam     | adam       |
| epochs                     | 10         | 10         | 5      | 1000       | 1          | 50         | 100      | 15         |
| learning rate              | 3e-4       | 1e-3       | 2e-4   | 3e-4       | 3e-4       | 3e-4       | 3e-4     | 1e-3       |
| use critic                 | True       | True       | True   | True       | True       | True       | True     | True       |
| epochs critic              | 10         | 10         | 5      | 1000       | 1          | 50         | 100      | 50         |
| learning rate critic       | 3e-4       | 1e-3       | 2e-4   | 3e-4       | 3e-4       | 3e-4       | 3e-4     | 5e-5       |
| number minibatches         | 32         | n.a.       | n.a.   | n.a.       | n.a.       | n.a.       | n.a.     | n.a.       |
| batch size                 | n.a.       | 500        | 1024   | 256        | 512        | n.a.       | n.a.     | 256        |
| buffer size                | n.a.       | n.a.       | n.a.   | 1e6        | 2e6        | n.a.       | n.a.     | 3000       |
| learning starts            | 0          | 0          | n.a.   | 10000      | 1e5        | 0          | 0        | 2          |
| polyak_weight              | n.a.       | n.a.       | n.a.   | 5e-3       | 5e-3       | n.a.       | n.a.     | 5e-3       |
| SDE sampling frequency     | n.a.       | 4          | n.a.   | n.a.       | n.a.       | n.a.       | n.a.     | n.a.       |
| entropy coefficient        | 0          | 0          | 0      | auto       | auto       | 0          | 0        | n.a.       |
| normalized observations    | True       | True       | False  | False      | False      | True       | False    | False      |
| normalized rewards         | True       | True       | 0.05   | False      | False      | False      | False    | False      |
| observation clip           | 10.0       | n.a.       | n.a.   | n.a.       | n.a.       | n.a.       | n.a.     | n.a.       |
| reward clip                | 10.0       | 10.0       | 10.0   | n.a.       | n.a.       | n.a.       | n.a.     | n.a.       |
| critic clip                | 0.2        | lin_0.3    | 10.0   | n.a.       | n.a.       | n.a.       | n.a.     | n.a.       |
| importance ratio clip      | 0.2        | lin_0.3    | 0.1    | n.a.       | n.a.       | n.a.       | n.a.     | n.a.       |
| hidden layers              | [128, 128] | [128, 128] | n.a.   | [256, 256] | [256, 256] | [128, 128] | [32, 32] | [128, 128] |
| hidden layers critic       | [128, 128] | [128, 128] | n.a.   | [256, 256] | [256, 256] | [128, 128] | [32, 32] | n.a.       |
| hidden activation          | tanh       | tanh       | relu   | relu       | relu       | relu       | relu     | leaky_relu |
| orthogonal initialization  | Yes        | No         | xavier | fanin      | fanin      | Yes        | Yes      | Yes        |
| initial std                | 1.0        | 0.5        | 1.0    | 1.0        | 1.0        | 1.0        | 1.0      | 1.0        |
| number of heads            | -          | -          | 4      | -          | -          | -          | -        | 8          |
| dims per head              | -          | -          | 16     | -          | -          | -          | -        | 16         |
| number of attention layers | -          | -          | 4      | -          | -          | -          | -        | 2          |
| max sequence length        | -          | -          | 5      | -          | -          | -          | -        | 1024       |

<sup>1</sup>Linear Schedule from 0.3 to 0.01 during the first 25% of the training. Then continued with 0.01.

Table 5: Hyperparameters for the Box Pushing Dense, Episode Length  $T = 100$ 

|                              | PPO        | gSDE       | GTrXL  | SAC        | PINK       | TCE        | BBRL       | TOP-ERL    |
|------------------------------|------------|------------|--------|------------|------------|------------|------------|------------|
| number samples               | 48000      | 80000      | 8000   | 8          | 8          | 152        | 152        | 4          |
| GAE $\lambda$                | 0.95       | 0.95       | 0.95   | n.a.       | n.a.       | 0.95       | n.a.       | n.a.       |
| discount factor              | 1.0        | 1.0        | 0.99   | 0.99       | 0.99       | 1.0        | 1.0        | 1.0        |
| $\epsilon_\mu$               | n.a.       | n.a.       | n.a.   | n.a.       | n.a.       | 0.05       | 0.1        | 0.005      |
| $\epsilon_\Sigma$            | n.a.       | n.a.       | n.a.   | n.a.       | n.a.       | 0.0005     | 0.00025    | 0.0005     |
| trust region loss coef.      | n.a.       | n.a.       | n.a.   | n.a.       | n.a.       | 1          | 10         | 1.0        |
| optimizer                    | adam       | adam       | adam   | adam       | adam       | adam       | adam       | adam       |
| epochs                       | 10         | 10         | 5      | 1          | 1          | 50         | 20         | 15         |
| learning rate                | 5e-5       | 1e-4       | 2e-4   | 3e-4       | 3e-4       | 3e-4       | 3e-4       | 3e-4       |
| use critic                   | True       | True       | True   | True       | True       | True       | True       | True       |
| epochs critic                | 10         | 10         | 5      | 1          | 1          | 50         | 10         | 30         |
| learning rate critic         | 1e-4       | 1e-4       | 2e-4   | 3e-4       | 3e-4       | 1e-3       | 3e-4       | 5e-5       |
| number minibatches           | 40         | n.a.       | n.a.   | n.a.       | n.a.       | n.a.       | n.a.       | n.a.       |
| batch size                   | n.a.       | 2000       | 1000   | 512        | 512        | n.a.       | n.a.       | 512        |
| buffer size                  | n.a.       | n.a.       | n.a.   | 2e6        | 2e6        | n.a.       | n.a.       | 7000       |
| learning starts              | 0          | 0          | 0      | 1e5        | 1e5        | 0          | 0          | 8000       |
| polyak_weight                | n.a.       | n.a.       | n.a.   | 5e-3       | 5e-3       | n.a.       | n.a.       | 5e-3       |
| SDE sampling frequency       | n.a.       | 4          | n.a.   | n.a.       | n.a.       | n.a.       | n.a.       | n.a.       |
| entropy coefficient          | 0          | 0.01       | 0      | auto       | auto       | 0          | 0          | 0.         |
| normalized observations      | True       | True       | False  | False      | False      | True       | False      | False      |
| normalized rewards           | True       | True       | 0.1    | False      | False      | False      | False      | False      |
| observation clip             | 10.0       | n.a.       | n.a.   | n.a.       | n.a.       | n.a.       | n.a.       | n.a.       |
| reward clip                  | 10.0       | 10.0       | 10.    | n.a.       | n.a.       | n.a.       | n.a.       | n.a.       |
| critic clip                  | 0.2        | 0.2        | 10.    | n.a.       | n.a.       | n.a.       | n.a.       | n.a.       |
| importance ratio clip        | 0.2        | 0.2        | 0.1    | n.a.       | n.a.       | n.a.       | n.a.       | n.a.       |
| hidden layers                | [512, 512] | [256, 256] | n.a.   | [256, 256] | [256, 256] | [128, 128] | [128, 128] | [256, 256] |
| hidden layers critic         | [512, 512] | [256, 256] | n.a.   | [256, 256] | [256, 256] | [256, 256] | [256, 256] | n.a.       |
| hidden activation            | tanh       | tanh       | relu   | tanh       | tanh       | leaky_relu | leaky_relu | leaky_relu |
| orthogonal initialization    | Yes        | No         | xavier | fanin      | fanin      | Yes        | Yes        | Yes        |
| initial std                  | 1.0        | 0.05       | 1.0    | 1.0        | 1.0        | 1.0        | 1.0        | 1.0        |
| number of heads              | -          | -          | 4      | -          | -          | -          | -          | 8          |
| dims per head                | -          | -          | 16     | -          | -          | -          | -          | 16         |
| number of attention layers   | -          | -          | 4      | -          | -          | -          | -          | 2          |
| max sequence length          | -          | -          | 5      | -          | -          | -          | -          | 1024       |
| Movement Primitive (MP) type | n.a.       | n.a.       | value  | n.a.       | n.a.       | ProDMPs    | ProDMPs    | ProDMPs    |
| number basis functions       | n.a.       | n.a.       | value  | n.a.       | n.a.       | 8          | 8          | 8          |
| weight scale                 | n.a.       | n.a.       | value  | n.a.       | n.a.       | 0.3        | 0.3        | 0.3        |
| goal scale                   | n.a.       | n.a.       | value  | n.a.       | n.a.       | 0.3        | 0.3        | 0.3        |

Table 6: Hyperparameters for the Box Pushing Sparse, Episode Length  $T = 100$ 

|                            | PPO        | gSDE       | GTrXL  | SAC        | PINK       | TCE        | BBRL       | TOP-ERL    |
|----------------------------|------------|------------|--------|------------|------------|------------|------------|------------|
| number samples             | 48000      | 80000      | 8000   | 8          | 8          | 76         | 76         | 4          |
| GAE $\lambda$              | 0.95       | 0.95       | 0.95   | n.a.       | n.a.       | 0.95       | n.a.       | n.a.       |
| discount factor            | 1.0        | 1.0        | 1.0    | 0.99       | 0.99       | 1.0        | 1.0        | 1.0        |
| $\epsilon_\mu$             | n.a.       | n.a.       | n.a.   | n.a.       | n.a.       | 0.05       | 0.1        | 0.005      |
| $\epsilon_\Sigma$          | n.a.       | n.a.       | n.a.   | n.a.       | n.a.       | 0.0005     | 0.00025    | 0.0005     |
| trust region loss coef.    | n.a.       | n.a.       | n.a.   | n.a.       | n.a.       | 1          | 10         | 1.0        |
| optimizer                  | adam       | adam       | adam   | adam       | adam       | adam       | adam       | adam       |
| epochs                     | 10         | 10         | 5      | 1          | 1          | 50         | 20         | 15         |
| learning rate              | 5e-4       | 1e-4       | 2e-4   | 3e-4       | 3e-4       | 3e-4       | 3e-4       | 3e-4       |
| use critic                 | True       | True       | True   | True       | True       | True       | True       | True       |
| epochs critic              | 10         | 10         | 5      | 1          | 1          | 50         | 10         | 30         |
| learning rate critic       | 1e-4       | 1e-4       | 2e-4   | 3e-4       | 3e-4       | 3e-4       | 3e-4       | 5e-5       |
| number minibatches         | 40         | n.a.       | n.a.   | n.a.       | n.a.       | n.a.       | n.a.       | n.a.       |
| batch size                 | n.a.       | 2000       | 1000   | 512        | 512        | n.a.       | n.a.       | 512        |
| buffer size                | n.a.       | n.a.       | n.a.   | 2e6        | 2e6        | n.a.       | n.a.       | 7000       |
| learning starts            | 0          | 0          | 0      | 1e5        | 1e5        | 0          | 0          | 400        |
| polyak_weight              | n.a.       | n.a.       | 0      | 5e-3       | 5e-3       | n.a.       | n.a.       | 5e-3       |
| SDE sampling frequency     | n.a.       | 4          | 0      | n.a.       | n.a.       | n.a.       | n.a.       | n.a.       |
| entropy coefficient        | 0          | 0.01       | 0      | auto       | auto       | 0          | 0          | 0          |
| normalized observations    | True       | True       | False  | False      | False      | True       | False      | False      |
| normalized rewards         | True       | True       | 0.1    | False      | False      | False      | False      | False      |
| observation clip           | 10.0       | n.a.       | False  | n.a.       | n.a.       | n.a.       | n.a.       | n.a.       |
| reward clip                | 10.0       | 10.0       | 10.0   | n.a.       | n.a.       | n.a.       | n.a.       | n.a.       |
| critic clip                | 0.2        | 0.2        | 10.0   | n.a.       | n.a.       | n.a.       | n.a.       | n.a.       |
| importance ratio clip      | 0.2        | 0.2        | 0.1    | n.a.       | n.a.       | n.a.       | n.a.       | n.a.       |
| hidden layers              | [512, 512] | [256, 256] | n.a.   | [256, 256] | [256, 256] | [128, 128] | [128, 128] | [256, 256] |
| hidden layers critic       | [512, 512] | [256, 256] | n.a.   | [256, 256] | [256, 256] | [256, 256] | [256, 256] | n.a.       |
| hidden activation          | tanh       | tanh       | relu   | tanh       | tanh       | leaky_relu | leaky_relu | leaky_relu |
| orthogonal initialization  | Yes        | No         | xavier | fanin      | fanin      | Yes        | Yes        | Yes        |
| initial std                | 1.0        | 0.05       | 1.0    | 1.0        | 1.0        | 1.0        | 1.0        | 1.0        |
| number of heads            | -          | -          | 4      | -          | -          | -          | -          | 8          |
| dims per head              | -          | -          | 16     | -          | -          | -          | -          | 16         |
| number of attention layers | -          | -          | 4      | -          | -          | -          | -          | 2          |
| max sequence length        | -          | -          | 5      | -          | -          | -          | -          | 1024       |
| MP type                    | n.a.       | n.a.       | value  | n.a.       | n.a.       | ProDMPs    | ProDMPs    | ProDMPs    |
| number basis functions     | n.a.       | n.a.       | value  | n.a.       | n.a.       | 8          | 8          | 8          |
| weight scale               | n.a.       | n.a.       | value  | n.a.       | n.a.       | 0.3        | 0.3        | 0.3        |
| goal scale                 | n.a.       | n.a.       | value  | n.a.       | n.a.       | 0.3        | 0.3        | 0.3        |

Table 7: Hyperparameters for the Hopper Jump, Episode Length  $T = 250$

|                            | PPO      | gSDE       | GTrXL  | SAC        | PINK     | TCE        | BBRL     | TOP-ERL    |
|----------------------------|----------|------------|--------|------------|----------|------------|----------|------------|
| number samples             | 8000     | 8192       | 10000  | 1000       | 1        | 64         | 64       | 1          |
| GAE $\lambda$              | 0.95     | 0.99       | 0.95   | n.a.       | n.a.     | 0.95       | n.a.     | n.a.       |
| discount factor            | 1.0      | 0.999      | 1.0    | 0.99       | 0.99     | 1.0        | 1.0      | 1.0        |
| $\epsilon_\mu$             | n.a.     | n.a.       | n.a.   | n.a.       | n.a.     | 0.1        | n.a.     | 0.1        |
| $\epsilon_\Sigma$          | n.a.     | n.a.       | n.a.   | n.a.       | n.a.     | 0.02       | n.a.     | 0.02       |
| trust region loss coef.    | n.a.     | n.a.       | n.a.   | n.a.       | n.a.     | 1          | n.a.     | 1.0        |
| optimizer                  | adam     | adam       | adam   | adam       | adam     | adam       | adam     | adam       |
| epochs                     | 10       | 10         | 10     | 1000       | 1        | 50         | 100      | 10         |
| learning rate              | 3e-4     | 9.5e-5     | 5e-4   | 1e-4       | 2e-4     | 1e-4       | 1e-4     | 1e-4       |
| use critic                 | True     | True       | True   | True       | True     | True       | True     | True       |
| epochs critic              | 10       | 10         | 10     | 1000       | 1        | 50         | 100      | 20         |
| learning rate critic       | 3e-4     | 9.5e-5     | 5e-4   | 1e-4       | 2e-4     | 1e-4       | 1e-4     | 5e-5       |
| number minibatches         | 40       | n.a.       | n.a.   | n.a.       | n.a.     | n.a.       | n.a.     | n.a.       |
| batch size                 | n.a.     | 128        | 1024   | 256        | 256      | n.a.       | n.a.     | 256        |
| buffer size                | n.a.     | n.a.       | n.a.   | 1e6        | 1e6      | n.a.       | n.a.     | 1000       |
| learning starts            | 0        | 0          | 0      | 10000      | 1e5      | 0          | 0        | 250        |
| polyak_weight              | n.a.     | n.a.       | n.a.   | 5e-3       | 5e-3     | n.a.       | n.a.     | 5e-3       |
| SDE sampling frequency     | n.a.     | 8          | n.a.   | n.a.       | n.a.     | n.a.       | n.a.     | n.a.       |
| entropy coefficient        | 0        | 0.0025     | 0.     | auto       | auto     | 0          | 0        | 0          |
| normalized observations    | True     | False      | False  | False      | False    | True       | False    | False      |
| normalized rewards         | True     | False      | False  | False      | False    | False      | False    | False      |
| observation clip           | 10.0     | n.a.       | False  | n.a.       | n.a.     | n.a.       | n.a.     | n.a.       |
| reward clip                | 10.0     | 10.0       | 10.    | n.a.       | n.a.     | n.a.       | n.a.     | n.a.       |
| critic clip                | 0.2      | lin_0.4    | 1.     | n.a.       | n.a.     | n.a.       | n.a.     | n.a.       |
| importance ratio clip      | 0.2      | lin_0.4    | 0.2    | n.a.       | n.a.     | n.a.       | n.a.     | n.a.       |
| hidden layers              | [32, 32] | [256, 256] | n.a.   | [256, 256] | [32, 32] | [128, 128] | [32, 32] | [128, 128] |
| hidden layers critic       | [32, 32] | [256, 256] | n.a.   | [256, 256] | [32, 32] | [128, 128] | [32, 32] | n.a.       |
| hidden activation          | tanh     | tanh       | relu   | relu       | relu     | leaky_relu | tanh     | leaky_relu |
| orthogonal initialization  | Yes      | No         | xavier | fanin      | fanin    | Yes        | Yes      | Yes        |
| initial std                | 1.0      | 0.1        | 1.0    | 1.0        | 1.0      | 1.0        | 1.0      | 1.0        |
| number of heads            | -        | -          | 4      | -          | -        | -          | -        | 8          |
| dims per head              | -        | -          | 16     | -          | -        | -          | -        | 16         |
| number of attention layers | -        | -          | 4      | -          | -        | -          | -        | 2          |
| max sequence length        | -        | -          | 5      | -          | -        | -          | -        | 1024       |
| MP type                    | n.a.     | n.a.       | value  | n.a.       | n.a.     | ProDMPs    | ProDMPs  | ProDMPs    |
| number basis functions     | n.a.     | n.a.       | value  | n.a.       | n.a.     | 3          | 3        | 3          |
| weight scale               | n.a.     | n.a.       | value  | n.a.       | n.a.     | 1          | 1        | 1          |
| goal scale                 | n.a.     | n.a.       | value  | n.a.       | n.a.     | 1          | 1        | 1          |